

Journal of Visualized Experiments

Noninvasive monitoring of lesion size in a heterologous mouse model of endometriosis --Manuscript Draft--

Article Type:	Invited Methods Article - JoVE Produced Video
Manuscript Number:	JoVE58358R3
Full Title:	Noninvasive monitoring of lesion size in a heterologous mouse model of endometriosis
Keywords:	endometriosis; non-invasive monitoring; animal model; fluorescence labeled lesions; endometriosis progression; heterologous mouse model of endometriosis
Corresponding Author:	R Dr. Gomez
Corresponding Author's Institution:	
Corresponding Author E-Mail:	raulgomgal@gmail.com
Order of Authors:	Jessica Martinez Viviana Bisbal Nerea Marin Antonio Cano Raul Gomez
Additional Information:	
Question	Response
Please indicate whether this article will be Standard Access or Open Access.	Standard Access (US\$2,400)
Please indicate the city, state/province, and country where this article will be filmed . Please do not use abbreviations.	Carrer d'Eduardo Primo Yúfera, 3, 46012 and Avenida de Menéndez y Pelayo, 4, 46010 Valencia, both of them in SPAIN

TITLE:

Noninvasive Monitoring of Lesion Size in a Heterologous Mouse Model of Endometriosis

AUTHORS & AFFILIATIONS:

Jessica Martínez¹, Viviana Bisbal², Nerea Marín², Antonio Cano^{1,3,4}, Raúl Gómez¹

¹ Instituto de Investigación Sanitaria, INCLIVA, Valencia, Spain

² Unidad de Animalario del Centro de Investigación Príncipe Felipe (CIPF), Valencia, Spain

³ Departamento de Pediatría, Obstetricia y Ginecología, Universidad de Valencia, Spain

⁴ Servicio de Obstetricia y Ginecología, Hospital Clínico Universitario de Valencia, Spain

Corresponding Author:

Raul Gómez (raulgomgal@gmail.com)

Author Email Addresses:

Jessica Martinez (jessik_nenu@hotmail.com)

Vibiana Bisbal (vbisbal@cipf.es)

Nerea Marín (nmarin@cipf.es)

Antono Cano (Antonio.cano@uv.es)

KEYWORDS:

Endometriosis, heterologous, mouse model, mCherry, in vivo, monitoring

SHORT ABSTRACT:

Here, we present a protocol for live-imaging of fluorescently labeled human endometrial fragments grafted in mice. The method allows studying the effects of drugs of choice on endometriotic lesion size through monitoring and quantification of fluorescence emitted by the fluorescent reporter on real time

LONG ABSTRACT:

Here, we describe a protocol for the implementation of a heterologous mouse model in which progression of endometriosis can be assessed in real time through noninvasive monitoring of fluorescence emitted by implanted ectopic human endometrial tissue. For this purpose, biopsies of human endometrium are obtained from donor women ongoing oocyte donation. Human endometrial fragments are cultured in the presence of adenoviruses engineered to express cDNA for the reporter fluorescent protein mCherry. Upon visualization, labeled tissues with an optimal rate of fluorescence after infection are subsequently chosen for the implantation in recipient mice. One week prior to the implantation surgery, recipient mice are oophorectomized, and estradiol pellets are placed subcutaneously to sustain the survival and growth of lesions. On the day of surgery mice are anesthetized, and peritoneal cavity accessed through a small (1.5 cm) incision by the *linea-alba*. Fluorescently labeled implants are tweezed, briefly soaked in glue and attached to the peritoneal layer. Incisions are sutured, and animals left to recover for a couple of days. Fluorescence emitted by endometriotic implants is usually non-invasively monitored every 3 days for 4 weeks with an *in vivo* imaging system. Variations in

the size of endometriotic implants can be estimated in real time by quantification of the mCherry signal and normalization against the initial time-point showing maximal fluorescence intensity.

Traditional preclinical rodents of models of endometriosis do not allow non-invasive monitoring of lesion in real time but rather allow evaluation of the effects of drugs assayed at the end point. This protocol allows one to track lesions in real time and is more useful to explore the therapeutic potential of drugs in preclinical models of endometriosis. The main limitation of the model thus generated is that non-invasive monitoring is not possible over long periods of time due to the episomal expression of Ad-virus.

INTRODUCTION:

Endometriosis is a chronic gynecologic disorder initiated by the implantation of the functional endometrium outside the uterine cavity. Ectopic lesions grow and induce inflammatory processes leading to chronic pelvic pain and infertility¹. It is estimated that up to 10%–15% of women of reproductive age are affected by endometriosis², and it is present in approximately 40-50% of infertile women³. Current pharmacological treatments for endometriosis are unable to completely eradicate lesions and not free of side effects^{4,5}. The research for more efficient therapies requires of the refinement of the existing animal models of endometriosis in such a way that human lesions can be appropriately mimicked, and the effects of compounds on lesion size among others can be closely assessed.

Primate models have been used to mimic endometriosis by implanting ectopic lesions histologically identical and at similar sites as in humans⁶⁻⁸; however, ethical concerns and the high economic costs related to experimentation with primates limit their use⁹. Consequently, the use of small animals, especially rodents, for the implementation of in-vivo models of endometriosis continues to be favored as it allows studies with larger numbers of individuals^{10,11}. Endometriosis can be induced in these animals by transplanting either pieces of rodent uterine horns ("homologous models")^{12,13} or human endometrial/endometriotic tissue to ectopic sites (heterologous models)¹⁴. In contrast to humans, rodents do not shed their endometrial tissue and thereby endometriosis can not be developed spontaneously in these species. Therefore, homologous mouse models of endometriosis have been criticized due to the fact that implanted ectopic mouse uterine tissue does not reflect the characteristics of human endometriotic lesions¹⁵.

Appropriate physiology of endometriosis can be mimicked in the heterologous models of endometriosis where fresh human endometrial fragments are implanted into immunodeficient animals. In conventional heterologous models, the therapeutic effects of compounds of interest are commonly assessed at the end point by the assessment of lesion size with the use of calipers¹⁶. An obvious limitation is that, as such, endpoint animal models do not allow studying implantation dynamics or endometriotic lesion development over time. An additional limitation is that the use of calipers does not allow accurate measurements of lesion size. Indeed, the standard error provided by calipers is in the same range (*i.e.*, millimeters) as the size of the lesions implanted in mice, thus restricting the capacity of these tools to detect actual variations

in size.

In order to overcome such limitations, herein, we describe the generation of a heterologous mouse model of endometriosis in which implanted human tissue is engineered to express a reporter m-Cherry fluorescent protein. Detection of the fluorescent signal with an appropriate image system enables non-invasive monitoring of lesion status with simultaneous quantification of its size in real time. Thus, our model provides clear advantages when compared to conventional endpoint models as it brings the opportunity of real-time non-invasive monitoring and the possibility to perform more objective and accurate estimation of variations in lesion size.

PROTOCOL:

The use of human tissue specimens was approved by the Institutional Review Board and Ethics Committee of the Hospital Universitario La Fe. All patients provided written informed consent. The study involving animals was approved by the Institutional Animal Care Committee at the Centro de Investigacion Principe Felipe de Valencia, and all procedures were performed following the guidelines for the care and use of mammals from the National Institutes of Health.

1) Endometrial Tissue Collection and Pre-Processing

1.1) Obtain a good quality biopsy of human endometrial aspirate by using a cannula attached to a suction device. Pour the biopsy into a flask containing 10 mL of sterile saline and wash with gentle manual agitation.

Note: Procedures on how to obtain good quality biopsies have been previously described¹⁷.

1.2) Wash the biopsy of any remaining blood or mucus. Repeat the process by pouring the tissue to flasks containing fresh saline as many times as required until tissue is observed clean.

1.3) Transfer biopsy fragments with a healthy appearance into a solution containing 10 mL of complete Dulbecco's Modified Eagle's medium (DMEM) medium with 10% Fetal Bovine Serum (FBS) and 1% antibiotic-antimycotic solution.

1.4) Pour the content in a 10 cm Petri dish and proceed to chop the tissue into 5-10 mm³ pieces with a pair of scalpels.

2) Adenoviral Transfection of Endometrial Fragments.

Note: All the materials that are going to be employed in the process should be introduced in the hood in advance. Take out everything that is not going to be used in the process and place a flask with bleach. All material that comes into contact with the adenoviral vector must be disinfected with the bleach before discarding it in the biohazard container.

2.1) Once the biopsy has been chopped, take a new Petri dish. Pipette multiple 30-50 μ L DMEM drops of spread throughout the whole dish. Leave enough space between drops so they do not come into contact.

2.2) Aided with a needle attached to syringe, place a single piece of fragment inside each of the medium drops.

Note: Each drop should contain a single piece of endometrium.

2.3) Prepare the Ad-mCherry working solution by diluting 1:20 of the mCherry adenoviral stock solution [$1 \cdot 10^{10}$ ifu/mL]) into DMEM medium WITHOUT antibiotics (DMEM + 10% filtered FBS).

2.4) Dispense 100-200 μ L of the Ad-mCherry solution per well on a 96-well plate, filling as many wells as fragments are available in the Petri dish drops (step 2.2). In addition, fill at least 3 wells with adenovirus free DMEM medium as a negative control.

2.5) Aided with a needle attached to syringe, transfer each of the fragments in the Petri dish (step 2.2) to each of the wells containing ad-mCherry solution in the 96-well plate.

2.6) Place the 96 well-plate containing the endometrial fragments with Ad-mCherry solution into an incubator at 37 °C with 5% CO₂ for 16 h.

2.7) Wash out the remaining adenoviruses in the medium by transferring tissues into a new 96-well plate filled with complete DMEM medium (WITH antibiotics-antimycotics, free of adenovirus) and incubate for 37 °C with 5% CO₂ for 24-48 h.

NOTE: Remember to cover with bleach all well plates and tips that came in contact with Ad-virus before discarding into the biohazard container.

2.8) Take out the plate from the incubator and place it under a fluorescence microscope at 568 nm (red channel) to test for optimal labeling.

2.9) Choose the most brilliant fragments and place them into a new 96-well plate with fresh complete DMEM medium (WITH antibiotics-antimycotics, free of adenovirus).

2.10) Seal the plate well with a plastic paraffin film and transport it to into the specific-pathogen-free animal area for implantation of endometrial fragments into recipient animals.

3) Generation of the Endometriosis Mouse Model

NOTE: Use 6-8-week-old athymic nude (or similar immunocompromised strains) female mice housed in specific pathogen-free conditions, as recipient animals. To avoid hormonal cycle-

dependent variations and simultaneously fuel lesion growth with estradiol, animals are ovariectomized and placed with 60-day release capsules containing 18 mg of 17 β -Estradiol (17 β -E₂). Oophorectomy and pellet placement have to be performed at least one week in advance of grafting endometrial fragments into the recipient animals.

3.1) Oophorectomy

Note: Prepare surgical sterilized material in a hood. Prepare anesthesia equipment and a post-surgical recovery zone ready in the same room.

3.1.1) Perform a subcutaneous injection of morphine derivative at a dose of 5 mg/kg per mouse. Let the mice rest for 30 min after injection so as analgesics effects of drug can be manifested.

3.1.2) Connect the inhalation anesthesia equipment and let oxygen and isoflurane (2% mg/kg) flow for a few min into a sealed anesthesia chamber.

3.1.3) Introduce the animal into the isoflurane anesthesia chamber. Wait for 3-5 min and check that animals are fully anesthetized by pressing one of its paws. Transfer the animal to the surgery area and maintain anesthesia by placing a mask with continuous flow of isoflurane gas covering the respiratory airways.

3.1.4) After disinfecting the area with chlorohexidine, perform a transverse 0.5 cm costal incision approximately at the height of the hip with sharp scissors.

3.1.5) Separate the skin from the muscle to get access to the abdominal cavity, identify the white fat pad that surrounds the ovary and retract the ovary with dissection forceps.

3.1.6) Tie a knot around the oviduct with absorbable suture and tighten it to ensure appropriate hemostasis before excising the ovary.

3.1.7) Close the muscular layer with 6-0 absorbable suture, and then close the skin with 6-0 non-absorbable suture. Clean the area again with antiseptic solution.

3.1.8) Repeat the procedure to remove the contra lateral ovary.

3.2) Estradiol pellet implant

Note: Take care that the animal is anesthetized during the oophorectomy surgery to place pellets at that point.

3.2.1) Immediately after the completion of the oophorectomy procedure, clean the skin with antiseptic solution surrounding the neck and make a transverse subcutaneous small (0.5 cm) incision with sharp scissors in the nape.

3.2.2) Use the scissors to dissect the skin from the muscle, making a pocket large enough to allow placing the pellets.

3.2.3) Insert the pellet containing 18 mg of 17β -E₂ and suture the skin with a 6-0 non-absorbable suture. Clean the area again with antiseptic solution.

3.2.4) Place the animal in the recovery zone and administer an optimal dose of long-lasting analgesia to ease the recovery period.

3.3) Endometrial implant surgery

NOTE: Allow at least a period of seven days quarantine to allow full recovery of animals after oophorectomy before starting endometrial fragment implantation surgery. For optimal synchronization with labeling of tissue, collect the biopsy 2-3 days before implantation surgery so as to avoid long-term culture of explants.

3.3.1) Get the surgical room in the specific pathogen free zone ready in advance. Prepare the hood with all required surgical material, the anesthesia equipment and the post-surgical recovery zone also.

3.3.2) Bring the animals to the room, perform a subcutaneous injection of a morphine derivative at a dose of 5 (mg/kg) in each mouse. Let the mice rest for 30 min after injection so analgesics effects of drug can be manifested.

3.3.3) Connect the inhalation anesthesia equipment and let oxygen and isoflurane (2% mg/kg) flow for a few min into a sealed anesthesia chamber.

3.3.4) Before starting surgery, move the plate containing fluorescently labeled fragments (from step 2.10) into the hood, unseal it and pour the fragments into a Petri dish for easier handling.

3.3.5) Introduce the animal into the isoflurane anesthesia chamber. Wait for 3-5 min and check that animals are fully anesthetized by pressing one of its paws. Transfer the animal to the surgery area and maintain anesthesia by placing a mask with continuous flow of isoflurane gas covering the respiratory airways.

3.3.5) Place the anesthetized animal face up. Disinfect the ventral area. Perform a longitudinal 1.5 cm incision in abdomen with sharp scissors and separate the skin from the muscle. Then, perform a longitudinal 1.5 cm incision in the muscle to access the peritoneal cavity.

3.3.6) Hold the left edge of the abdomen muscular wall with mini-forceps and fold it trying to expose the inner face of the peritoneum on the outside.

3.3.7) Take an endometrial implant with mini tweezers, soak it briefly in an n-butyl-ester cyanoacrylate adhesive and place it to the peritoneum where it will get attached. Let it dry for a few seconds. Repeat steps 3.3.6 and 3.3.7 to place an implant on the contralateral side of the peritoneum.

3.3.8) Close the muscular layer with an absorbable 6-0 suture, and then close the skin with a non-absorbable 6-0 suture. Clean the area again with antiseptic solution.

3.3.9) Place the animal in the recovery zone and administer an optimal dose of long-lasting analgesia.

4) ***In Vivo* Fluorescent Imaging with an *in vivo* imaging system**

4.1) Turn on the *in vivo* imaging system device, initialize the program and allow the CCD camera to cool down for a few min.

4.2) Prepare the inhalation anesthesia equipment. Open the isoflurane flow at 2% for a couple of min to fill the anesthetic chamber. Prepare the post-anesthesia recovery zone.

4.3) Once the program has started and the CCD camera have cooled down, click the **Imaging Wizard** tool: A tutorial starts with a series of consecutive windows displayed, each one corresponding to a parameter of interest with several options available to be chosen by clicking in the corresponding box. Move forward through the tutorial by selecting the appropriate boxes in each window and click the **OK** button to move to the next set of parameters with the following sequence.

4.3.1.) Select the **Epiluminescence box** for the fluorescence parameter, select the **mCherry box** for the filter pairs parameter. Check the **Photograph mode** and **Confirm Focus** boxes and select the Automatic box for the exposure parameter.

4.4) Once the instrument has been set up, move one animal inside the anesthesia chamber. When fully anesthetized, transfer the animal inside the *in vivo* imaging system cage and place it side up with its head inside a tubule connected to the anesthesia machine. Close the lid and click **Acquire** for monitoring.

4.5) Acquire the images appearing (a total of five images, one image for each pair of filters selected) and save data by clicking the **Save As** button. Move the mouse to the area of post-anesthesia recovery. Repeat the process with the remaining animals.

4.6) Repeat monitoring two or three times a week to follow-up the signal appropriately during the time course.

4.7) Proceed to sacrifice the animal at the end of the time course by CO₂ asphyxiation.

5) Quantification of *In Vivo* Fluorescence Images

5.1) Segregation of actual fluorescence through image unmixing:

5.1.1) Open the *In Vivo* Imaging Analysis Coupled Software Program.

5.1.2) Choose the “Sequenceinfo” file to start the analysis. Two windows will appear: “Sequence view” and “Tool Palette”. Choose **Tool Palette** and once the menu has been displayed select the following options.

5.1.3) Select **Corrections** and click on the box **Adaptive FL Background Subtraction** to remove the undesirable fluorescent signals from the luminescent image data. Choose the threshold of greatest interest and click **Set**.

5.1.4.) Click **Spectral Unmixing**, select the wavelengths of interest, the method chosen for unmixing (library, guided, automatic or manual) and then click **Start Unmix**.

5.1.5) Select the **Unmixed** image corresponding to mCherry signal and double click. A new window will appear with the final image of the signal of interest.

5.1.6) Repeat step 5.1.3.

5.1.7) OPTIONAL: If a representative image (JPEG) of the unmix result is needed, choose the desired settings in **Tool Palette | Image Adjust** (color table, binning, contrast, etc.), and then click on **Export Graphics** in the unmix window to export the current image view as an image.

5.1.8) Save the unmixed file: **File | Save As | Choose Folder** and **Ok**.

5.1.9) Repeat the process with the rest of the monitoring days and with all animals.

5.2) ROIs set up and signal quantification

5.2.1) Click **Browse** and select the **Unmixed file** (see step 5.1.8) of interest to be analyzed. A new window will appear.

5.2.2) Click **Add To List** to include all the unmixed files from each animal at different time points and then click on **Load As A Group**. All images must appear as a single sequence.

5.2.3) Go to **Tool Palette** window: Click off the box **Individual** scale to obtain all images on the same scale.

5.2.4) Double click in one image of the sequence and create a ROI on the zone of interest using the following sequence. Go to **ROI Tools** and select **Countour** and **Auto 1** option, click on the circle shape appearing, place it on the center the fluorescent signal and then click **Create** on the

displayed window.

Note: This automatically highlights pixels with an intensity of fluorescence above background values (*i.e.*, lesion) and generates a shape whose area embraces the outlined pixels.

5.2.5) Copy the created ROI shape and paste on a background zone where there is no signal.

5.2.6) Click on **Measure ROIs | Select All** to display values of fluorescence intensity. Proceed to select data values with the mouse, click right button, press copy and paste on a spreadsheet.

6) Data (fluorescent signal) Normalization

6.1) Select the initial time point at which signal intensity is maximal. Proceed to normalize signal at each time point by using the formula:

Signal intensity at each time point / Maximal signal intensity observed during the time course) x 100.

REPRESENTATIVE RESULTS:

Here, we describe the process for creating a heterologous model of endometriosis in which the architecture of lesions is preserved by implanting fluorescently labeled pieces of human endometrium into immunocompromised mice, thus allowing non-invasive monitoring of lesion progression. Labeling of endometrial fragments is achieved by infection with adenovirus engineered to express mCherry, a protein emitting fluorescence in the near infrared region. In **Figure 1**, we show representative images of human endometrial fragments infected with Ad-mCherry observed under the fluorescence microscope. For illustrative purposes, both labeled and non-labeled fragments are included so differences in fluorescence between infected and non-infected tissues (autofluorescence) can be noted. During monitoring, in addition to the reference wavelength for mCherry, fluorescent images are taken with different pairs of excitation/emission wavelengths filters (**Figure 2**) to define the characteristic fluorescent emission profile of tissues. The purpose of this action is to “unmix” actual fluorescence emitted by lesions from background and autofluorescence emitted by host tissues and scar originated during surgery respectively. An illustrative example of the unmix process is shown in **Figure 3**. Estimations of variation in lesion size is performed by quantifying and normalizing fluorescent signaling emitted by lesions during the time course. For this purpose, images of monitoring containing raw fluorescence emitted by animals during each time point are first brought together unnormalized (**Figure 4**) in a single file. Subsequently fluorescence is unmixed, normalized and represented as a false color image (**Figure 5**). Finally, ROIs corresponding to specific lesion and background signaling are automatically recognized by the program and quantified (**Figure 6**). Background ROI signaling is subtracted from lesion ROI signaling and results of intensity in each time point are normalized against the time point at which intensity is maximal (**Figure 7**). At the end of the monitoring process, several weeks after surgery mice are sacrificed and viable implant can be recovered attached to the mouse peritoneum (**Figure 8**).

FIGURE AND TABLE LEGENDS:

Figure 1: Visualization of endometrial fragments with fluorescence microscope after Ad-mCherry infection **A)** Human endometrial fragment incubated with Ad-mCherry at 37 °C and 5% CO₂ during 24 h as a positive sample. **B)** Human endometrial fragment incubated at 37 °C and 5% CO₂ without Ad-mCherry as a negative control sample.

Figure 2: Raw imaging fluorescence emitted by labeled fragments implanted in mice. Picture shows representative imaging of raw fluorescence signal emitted by the same animal at a specific time point. Images correspond to screenshots obtained using software coupled to an *in vivo* imaging system device during a monitoring session. Each panel containing mice (numbered 1 - 5 in the left corner) corresponds to the fluorescence observed by using a different specific excitation/emission pair filter for acquiring images. Panel on the right (tool palette) show fluorescence parameters selected for acquisition of images

Figure 3: Unmixing of background vs specific fluorescence emitted by lesions. Picture shows representative images of the unmixing process performed to dissect actual fluorescence from lesions using the *in vivo* imaging system coupled software. Graph on the left panel denote normalized specific profiles of fluorescence emission by scar (green line, UMX1), lesions (red line, UMX2) and host tissue (blue line, UMX3 panel). Fluorescence intensity at different emission wavelengths (X-axis) is represented in units of radiant efficiency (Y-axis). Just note how each specific structure (*i.e.*, scar, labeled lesions and host tissue) emits a different fluorescence profile which allows identifying and segregating them specifically from each other. On the right panel, fluorescence arising from launching specific emission profiles for scar (UMX1), lesions (UMX2) and host tissue (UMX3) are shown superposed on photograph images of mice. A composite image (Composite) is also included for illustrative purposes to denote the segmentation of fluorescence emitted by lesions from that emitted by scar or host tissues. Middle panel shows parameters selected for unmixing with the image software coupled to the *in-vivo* imaging device

Figure 4. Time course monitoring of raw fluorescence emitted by lesions. Panel shows representative images of raw fluorescence emitted by a single mouse implanted with labeled human lesions (brilliant yellow spots) during the time course. Time points after surgery at which monitoring was performed are denoted as “Day (number)”. Emission and excitation pair filters used for monitoring are indicated in each panel/image. Each panel is identified by a specific code (BKG) in the upper part containing info related to the date at which fluorescence was acquired

Figure 5: Time course monitoring of normalized fluorescence emitted by lesions. Representative images corresponding to unmixed, normalized fluorescent signaling emitted by human lesions (spots with rainbow color) superposed in a single mouse during the time course (days after surgery). Time points after surgery at which monitoring was performed are denoted as “Day (number)”. Each panel is identified by a specific code (BKG) in the lower part containing info related to the date at which fluorescence was acquired. Rainbow palette color on the right

side identifies fluorescence intensity (Radiant efficiency) emitted by lesions at each time point. Note how strong fluorescence intensity during the initial time points (*i.e.*, red color in the center of lesions on days 1,5 and 8) declines during the time course (*i.e.*, blue color in lesions on days 20 and 25).

Figure 6: Use of ROIs for quantification of fluorescence intensity in lesions during the time course. Figure shows panel of images of normalized fluorescence emitted by lesions in a single mouse during the time course (*i.e.*, **Figure 5**) with the addition of ROIs (delineating lesions and background) for quantification of fluorescence intensity. ROI 1 and ROI 2 identify the amount of fluorescence emitted by each of the two lesions during the time course. BKG identify the amount of fluorescence emitted by the host tissue (background fluorescence) during the time course. Background fluorescence is subtracted from ROIs for quantification purposes. Time points after surgery at which monitoring was performed are denoted as “Day (number)”. Images acquired at each time point are labeled with a specific code (BKG) at the bottom of each one containing info related to the date at which fluorescence was acquired (first eight digits following BKG detail data for year(2014)-month (10) and -day(10 to 31)), an individual identification code (last 6 digits) and the specific profiles of fluorescence emission used for unmixing (UMX2) Rainbow palette color on the right side provides a visual scale of fluorescence intensity (Radiant efficiency) emitted by lesions at each time point. Note how fluorescence intensity values in the two lesions (ROI1 and ROI2) are higher at the initial time points (days 1 and 5) and decays during the time course to reach the lowest values at the end time points (days 20 and 25).

Figure 7: Normalization of fluorescence intensity during the time course. Table in the upper part shows illustrative example of the values of fluorescence intensity (radiant efficiency) emitted by two mCherry labeled lesions (ROI1 and ROI2) implanted in a mouse (R25). Monitoring of fluorescence was performed at different days after surgery (D5-D25) during the time course. D5- Graph at the bottom illustrates typical pattern of normalized fluorescence emitted by lesions infected with mCherry decaying during the time course. Y-axis shows values of fluorescence normalized to express the percentage of decay by using the formula (Signal intensity at each time point / Maximal signal intensity observed during the time course) x 100. Time points (Days (Dx) after implanting surgery) at which fluorescence was monitored are indicated in the X-axis. Note initial increase of signaling during the first 24 hrs after surgery, corresponding to stabilization of lesion, the peak in fluorescence intensity around D1-D5 and its subsequent decay due to episomal expression of mCherry during the time course

Figure 8: Macroscopic appearance of implanted endometriotic lesions. Representative images showing macroscopic appearance of endometriotic lesions implanted in mice at the end of the monitoring process upon sacrifice

DISCUSSION:

The protocol herein detailed describes the implementation of an animal model of endometriosis in which the architecture of implanting lesions architecture is preserved whilst simultaneously allowing real time assessment of fluorescence emitted by mCherry labeled

endometrial tissue. In this protocol, we describe the use of a specific *in vivo* imaging system and related software to non-invasively assess fluorescence emitted by the labeled lesion. Each user should adapt the protocol depending on the specific imaging device and related software available at their institution. Monitoring is performed in anesthetized animals through an isoflurane gas anesthesia machine coupled to an *in vivo* imaging system. To avoid interference with auto-fluorescence emitted by wounds, it is recommended to start monitoring lesions fluorescence at least three days after implantation surgery.

Heterologous mouse models of endometriosis similar to the one herein shown have been previously described consisting in the implantation endometrial fragments labeled with green fluorescent protein (GFP)^{18,19}. The use of mCherry as a reporter for tagging the human tissue provides however an advantage over GFP because of the enhanced tissue penetration of the former. Due to its larger emission spectrum and higher photostability mCherry emits a brighter signal that is more appropriate for the visualization of intraperitoneal fragments.

Due to its small size adenoviruses are the vectors of choice for infection (*i.e.*, labeling) of whole tissue pieces as those provide acceptable diffusion through 3D structures. Even with that the percentage of tissue infected cells is not higher than 30-35%. Thus, the limitation of this model relies on the inefficient labeling of tissue and additionally the transient expression achieved by adenoviruses. Indeed, fluorescence cannot be monitored beyond 4–6 week as it fades progressively due to the episomal transient expression of the Ad-virus. Efficiency of labeling and the period of monitoring might be increased by disrupting the donor tissue and infecting isolated single epithelial/stromal cells with ad-virus previous to being injected into recipient mice^{19,20}. Such an approach, however, reduces the extent at which the animal model mimics the physiology of endometriosis provided that ectopic human lesions do not consist in a disorganized accumulation of single epithelial/stromal cells but rather in well-structured endometriotic tissue.

In this protocol, the most critical step is the labeling of the tissue and most specifically the determination of the appropriate concentration of ad-virus required for optimal infection. Indeed, the 1×10^{10} pfu/mL concentration pointed out in the protocol is mostly an orientative/consensus figure based on our experience. The optimal concentration might differ in each experiment depending on the type and quality of the biopsy and/or how quickly this is processed. We thus suggest testing at least three different (two-fold) titers in each experiment and choosing the one providing optimal labeling based on visualization under the fluorescence microscope.

Our protocol/model is useful to study the mechanisms implicated in the establishment and early development of the endometriotic lesions. In spite of the period of time of monitoring is constrained, the model is still useful to study and detect the effects of pharmacological compounds able to exert dramatic effects on lesion size in a short period of time such as antiangiogenic or antiestrogenic drugs. The development of more efficient and durable methods of labeling human tissue are expected to spread non-invasive monitoring as a consolidated technique to explore the potential therapeutic of a wider range of drugs in

preclinical model endometriosis.

ACKNOWLEDGMENTS:

This work was supported by Spanish Ministry of Economy and Competitiveness through the Miguel Servet Program [CP13/00077] cofounded by FEDER (European Regional Development Fund) and awarded to Dr R. Gómez as well as by Carlos III Institute of Health grants awarded to Dr R Gómez [PI14/00547 and PI17/02329] and to Prof A. Cano [PI12/02582].

DISCLOSURES:

The authors have nothing to disclose.

REFERENCES:

1. Nap AW, Groothuis PG, Demir AY, Evers JL, Dunselman GA. Pathogenesis of endometriosis. *Best Practice & Research: Clinical Obstetrics & Gynaecology*; **18**, 233–244 (2004).
2. Holoch KJ, Lessey BA. Endometriosis and infertility. *Clinical Obstetrics and Gynecology*; **53**, 429–438 (2010).
3. Eskenazi B, Warner ML. Epidemiology of endometriosis. *Obstetrics and Gynecology Clinics of North America*; **24** (2), 235–258 (1997).
4. Giudice LC, Kao LC. Endometriosis. *Lancet*; **364** (9447), 1789–1799 (2004).
5. Donnez J, *et al.* The efficacy of medical and surgical treatment of endometriosis-associated infertility and pelvic pain. *Gynecologic and Obstetric Investigation*; **54**, 2–7 (2002).
6. D’Hooghe TM, Bambra CS, Cornillie FJ, Isahakia M, Koninckx PR. Prevalence and laparoscopic appearance of spontaneous endometriosis in the baboon (*Papio anubis*, *Papio cynocephalus*). *Biology of Reproduction*; **45** (3), 411–416 (1991).
7. Dick EJ, Hubbard GB, Martin LJ, Leland MM. Record review of baboons with histologically confirmed endometriosis in a large established colony. *Journal of Medical Primatology*; **32** (1), 39–47 (2003).
8. Donnez O, *et al.* Induction of endometriotic nodules in an experimental baboon model mimicking human deep nodular lesions. *Fertility & Sterility*; **99** (3), 783–789 (2013).
9. Grummer R. Animal models in endometriosis research. *Human Reproduction Update*; **12** (5), 641–649 (2006).
10. Rossi G, *et al.* Dynamic aspects of endometriosis in a mouse model through analysis of implantation and progression. *Archives of Gynecology and Obstetrics*; **263** (3), 102–107 (2000).
11. Grummer R, *et al.* Peritoneal endometriosis: validation of an in-vivo model. *Human Reproduction*; **16** (8), 1736–1743 (2001).
12. Becker CM, *et al.* A novel non-invasive model of endometriosis for monitoring the efficacy of antiangiogenic therapy. *The American Journal of Pathology*; **168** (6), 2074–2084 (2006).
13. Laschke MW, Giebels C, Nickels RM, Scheuer C, Menger MD. Endothelial progenitor cells contribute to the vascularization of endometriotic lesions. *The American Journal of Pathology*; **178** (1), 442–450 (2011).
14. Nap AW, *et al.* Antiangiogenesis therapy for endometriosis. *The Journal of Clinical Endocrinology & Metabolism*; **89** (3), 1089–95 (2004).

- 573 15. Wang CC, *et al.* Prodrug of green tea epigallocatechin-3-gallate (Pro-EGCG) as a potent
574 anti-angiogenesis agent for endometriosis in mice. *Angiogenesis*; **16** (1), 59–69 (2013).
- 575 16. Delgado-Rosas F, *et al.* The effects of ergot and non-ergot-derived dopamine agonists in
576 an experimental mouse model of endometriosis. *Reproduction*; **142** (5), 745-55 (2011).
- 577 17. Al-Jefout M, Andreadis N, Tokushige N, Markham R, Fraser I. A pilot study to evaluate
578 the relative efficacy of endometrial biopsy and full curettage in making a diagnosis of
579 endometriosis by the detection of endometrial nerve fibers. *American Journal of Obstetrics &*
580 *Gynecology*; **197** (6), 578 (2007).
- 581 18. Fortin M, *et al.* Quantitative assessment of human endometriotic tissue maintenance
582 and regression in a noninvasive mouse model of endometriosis. *Molecular Therapy*; **9** (4), 540-7
583 (2004).
- 584 19. Liu B, *et al.* Improved nude mouse models for green fluorescence human endometriosis.
585 *Journal of Obstetrics and Gynaecology Research*; **36** (6), 1214-21 (2010).
- 586 20. Wang N, *et al.* A red fluorescent nude mouse model of human endometriosis:
587 advantages of a non-invasive imaging method. *European Journal of Obstetric Gynecologic and*
588 *Reproductive Biology*; **176**, 25-30 (2014).
- 589

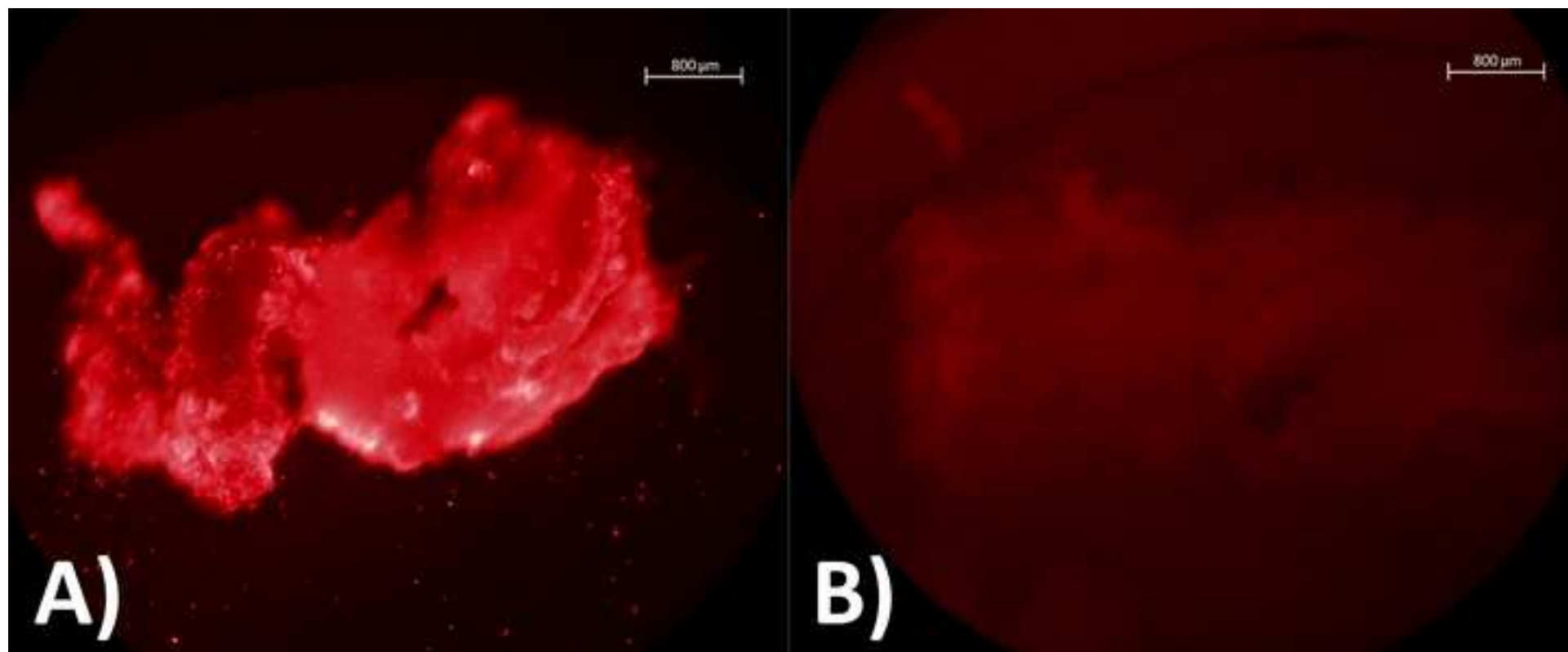


Figure 2

[Click here to download Figure Figure2 new.tif](#)

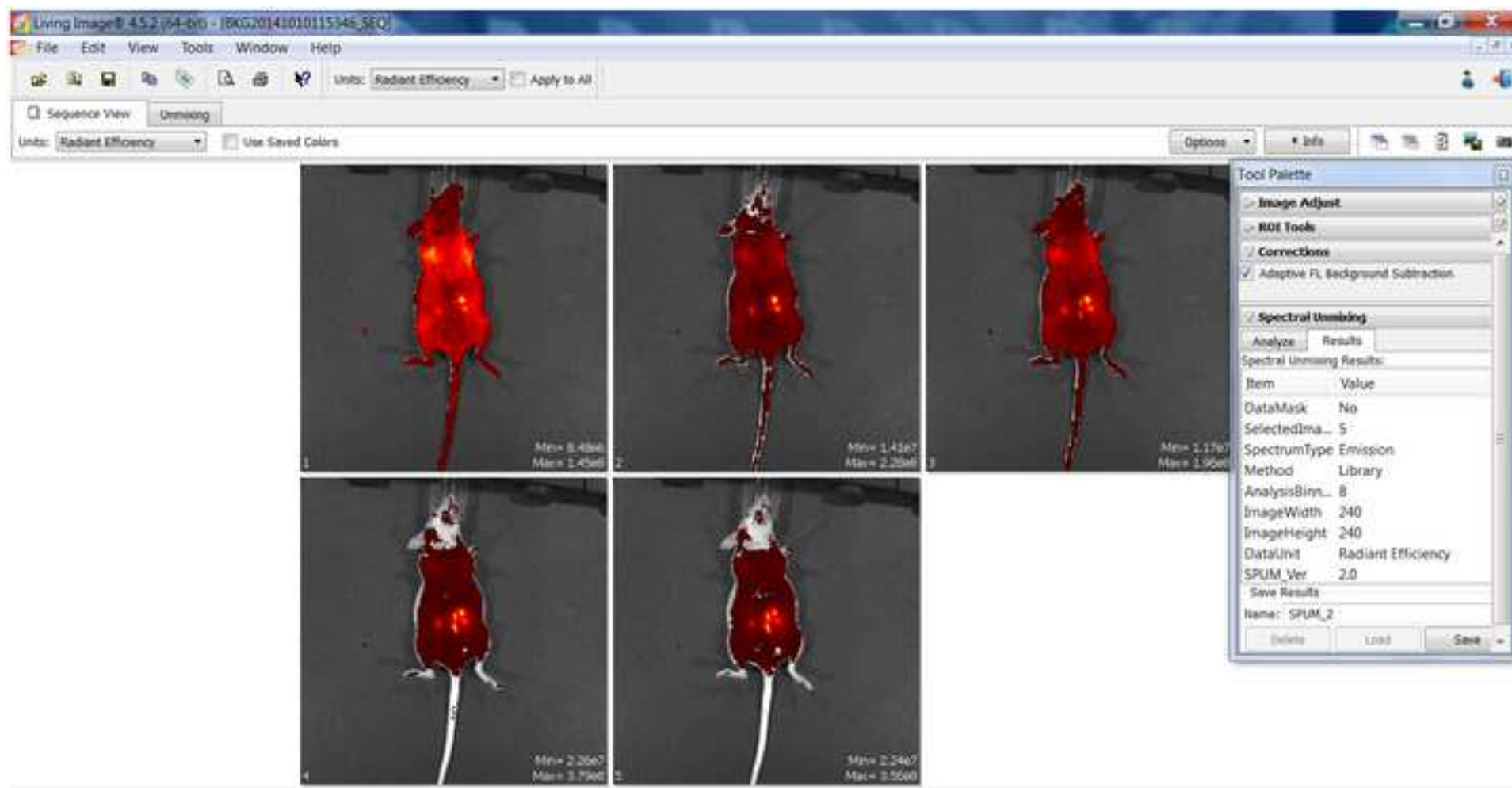


Figure 3

[Click here to download Figure Figure3-new.tif](#)



Figure 4

[Click here to download Figure Figure 4-news.tif](#)

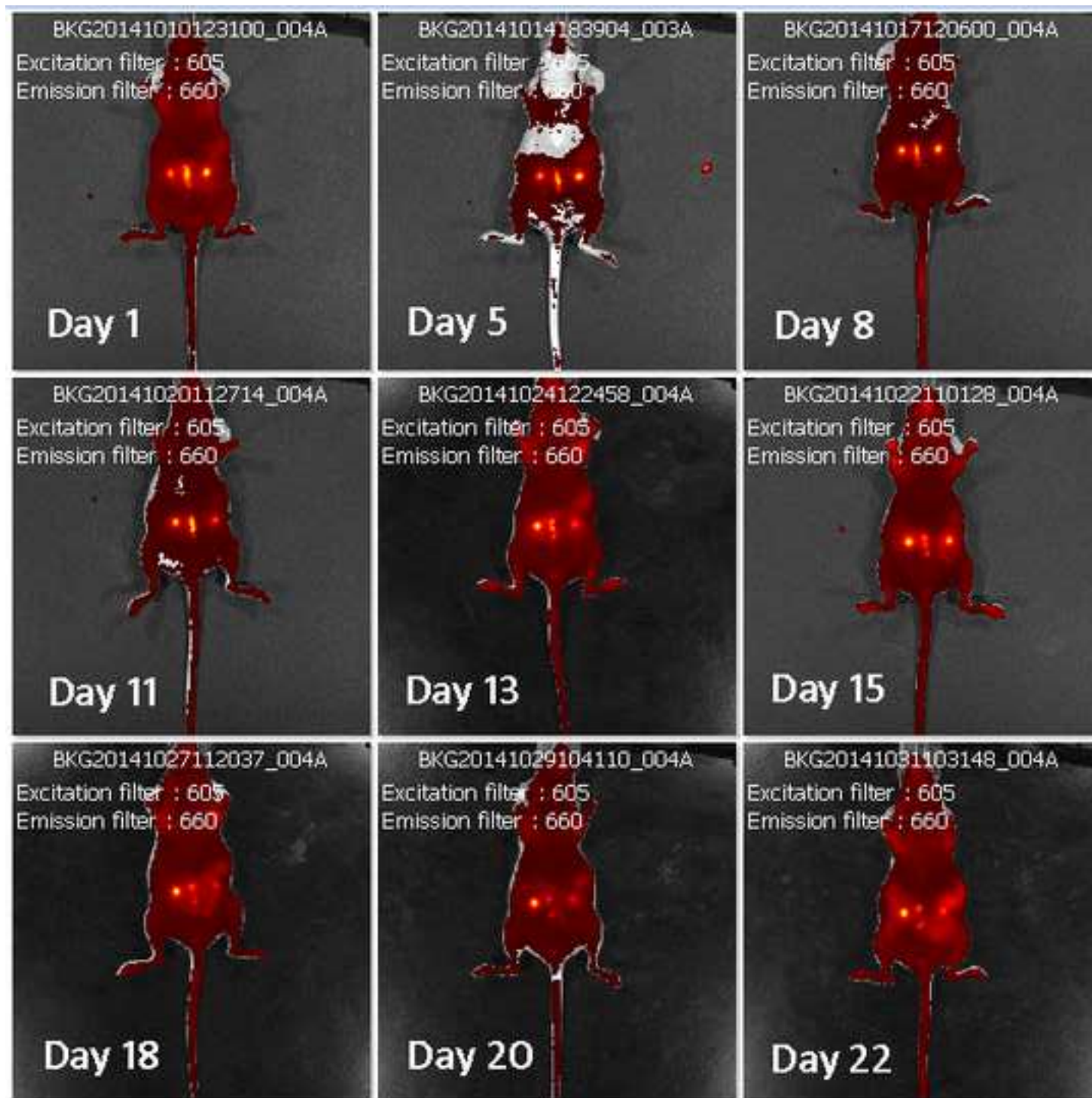


Figure 5

[Click here to download Figure Figure 5-news.tif](#)

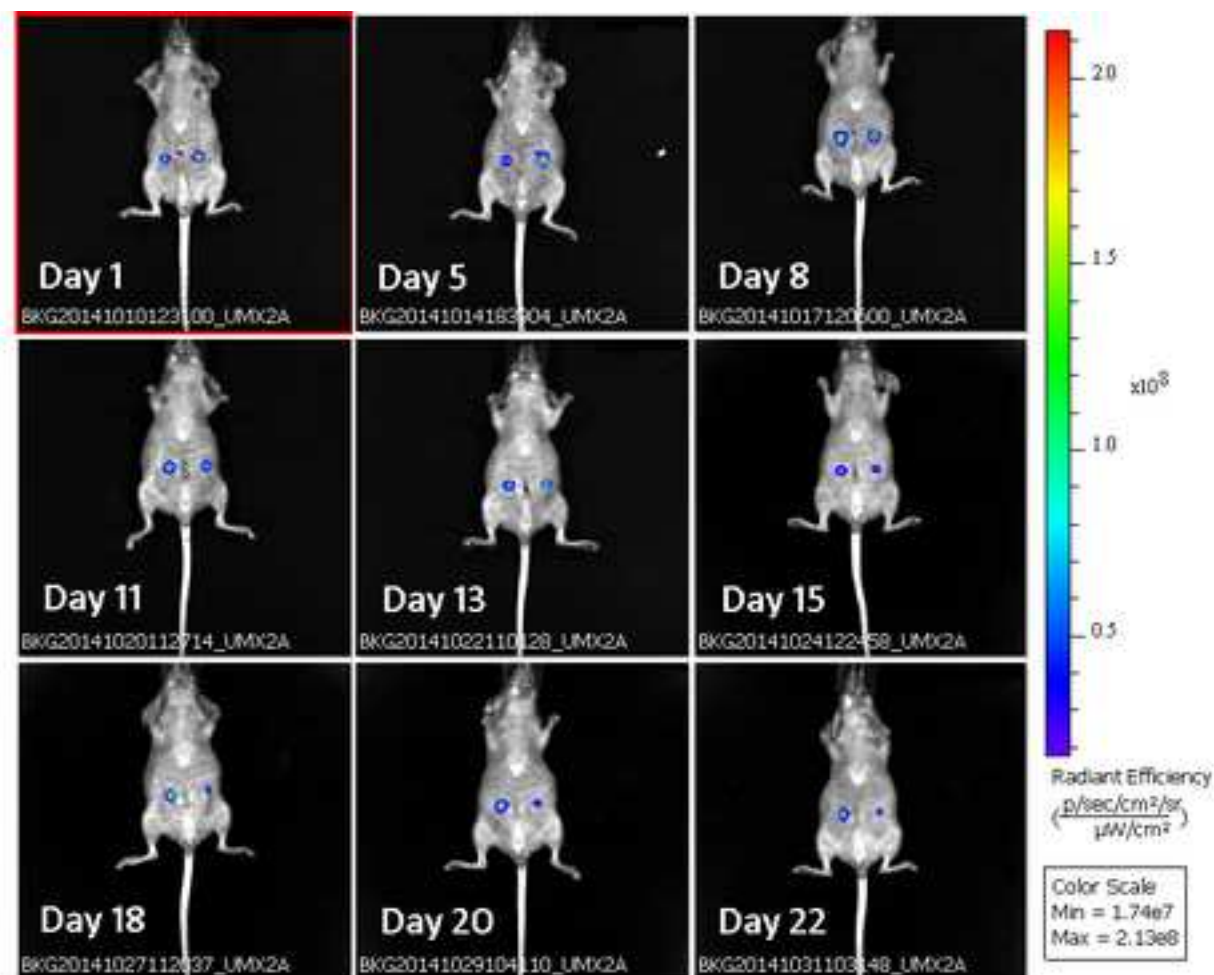
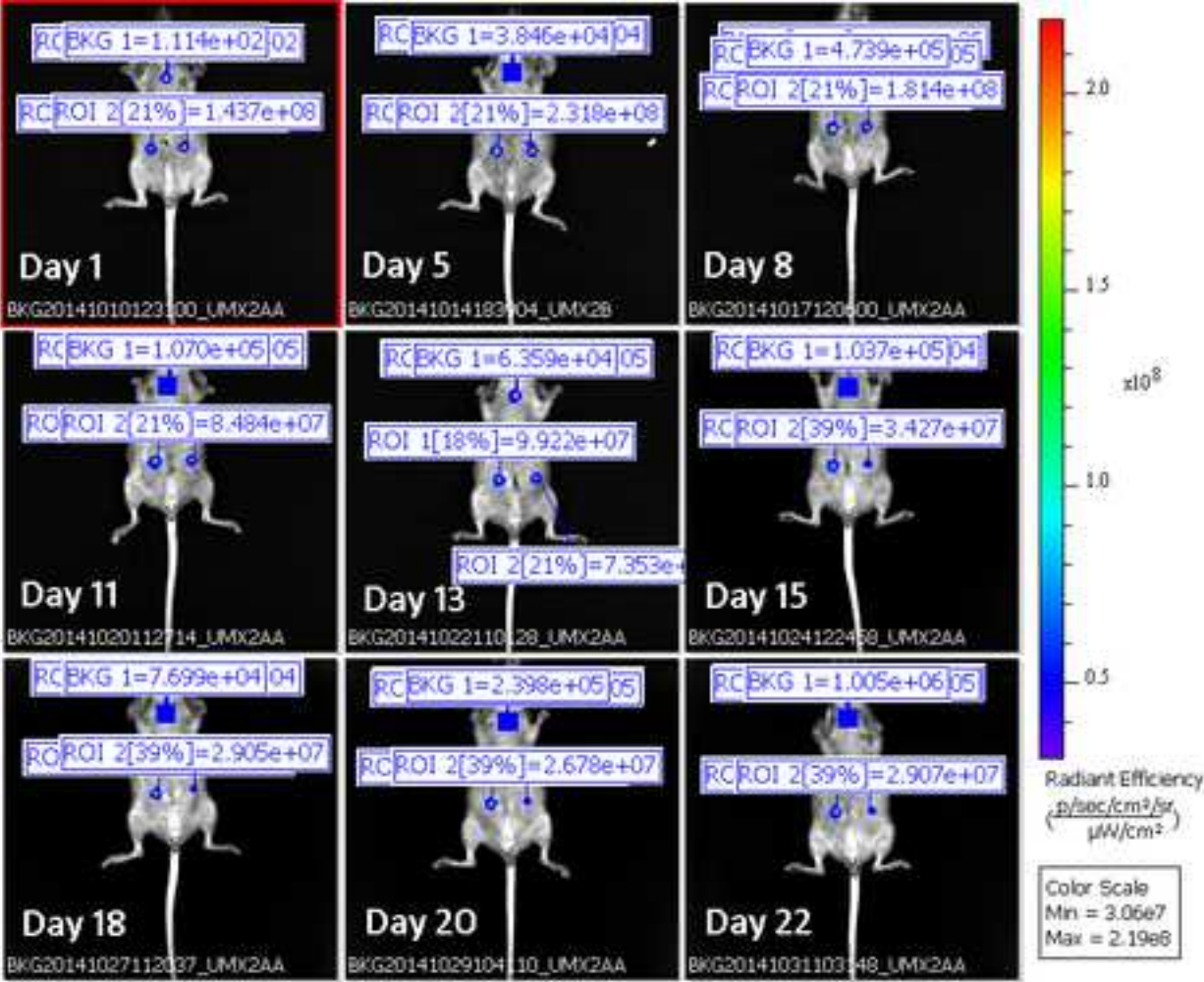


Figure 6



R25 - ROI	AVERAGE RADIANT EFFICIENCY							
	D5	D8	D11	D13	D15	D18	D20	D22
ROI1	8,35E+07	9,24E+07	5,11E+07	4,35E+07	3,97E+07	7,53E+07	7,80E+07	4,67E+07
ROI2	1,28E+08	1,07E+08	5,13E+07	4,80E+07	3,79E+07	3,52E+07	3,39E+07	3,60E+07

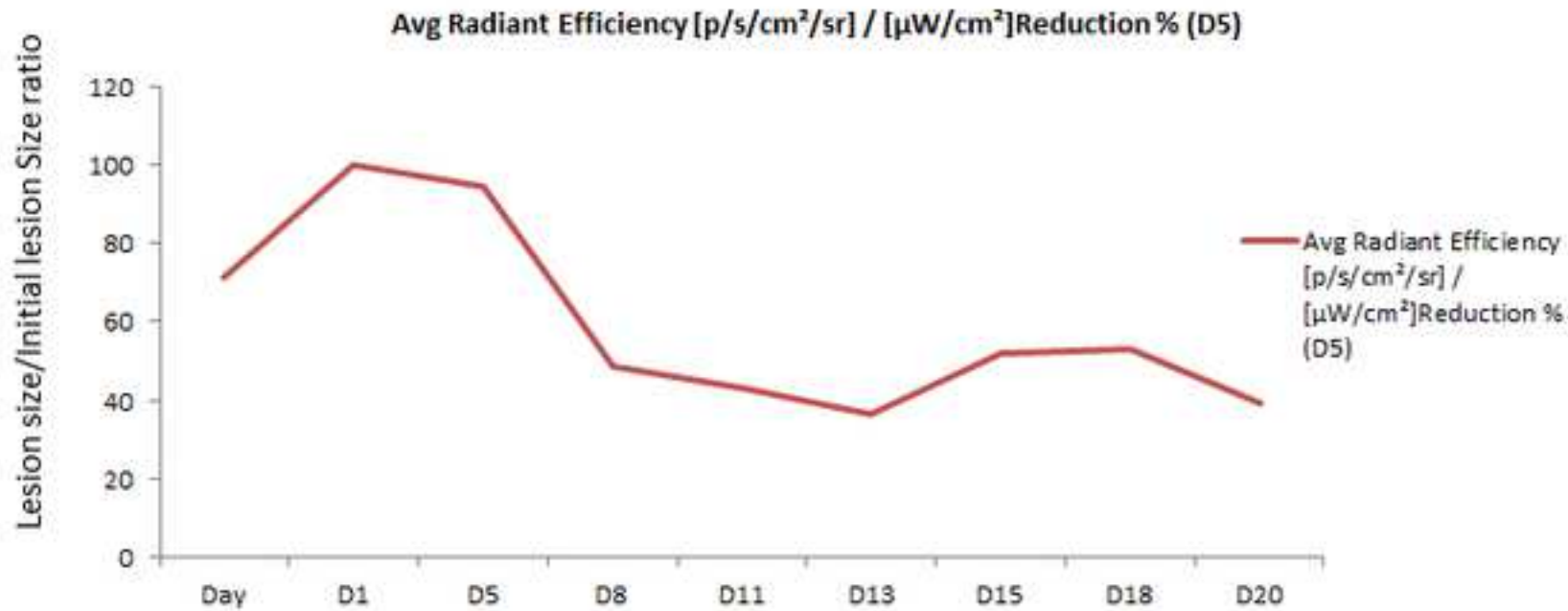
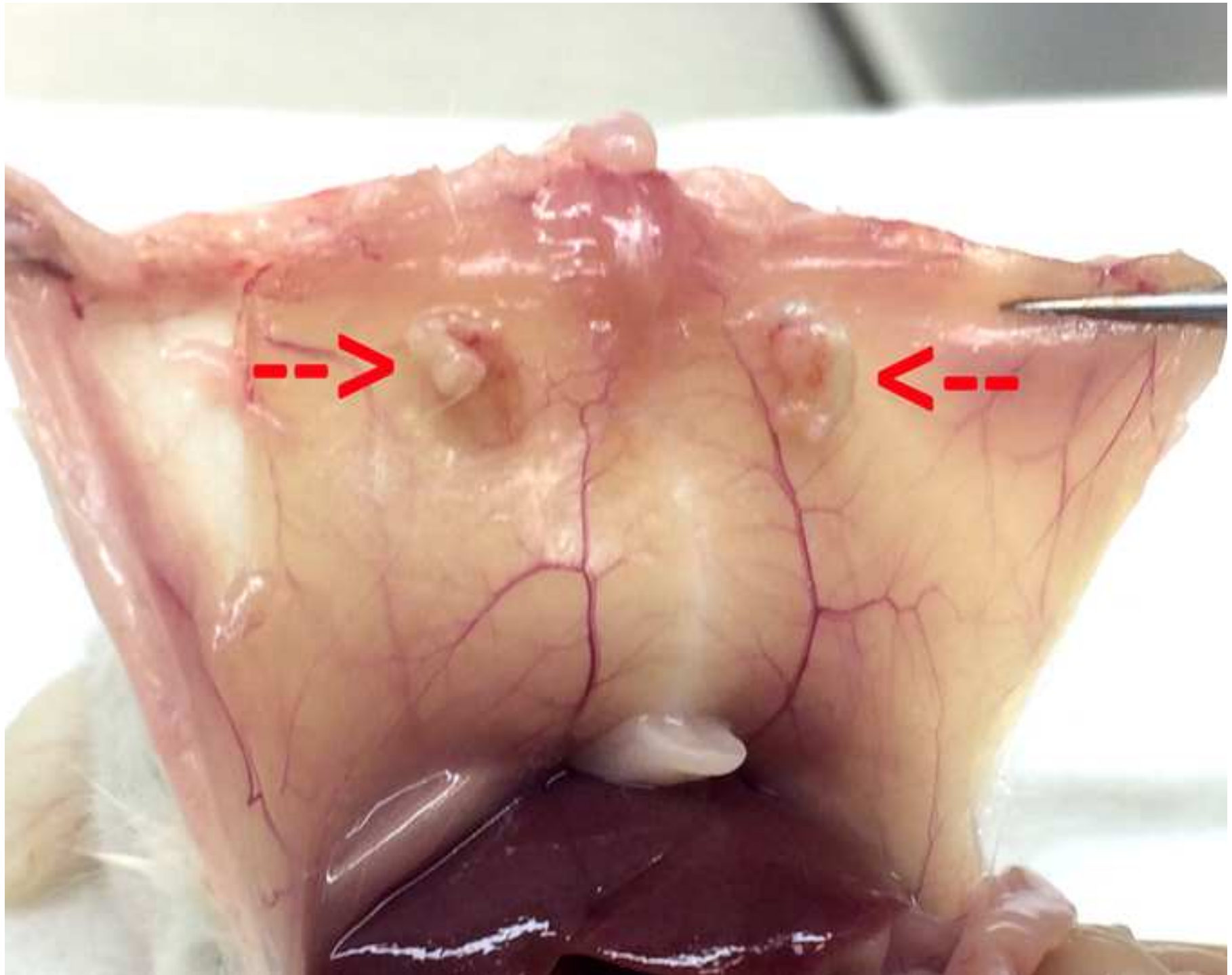


Figure 8



Name of Material/ Equipment	Company
Endosampler™	Medgyn
DMEM Medium	VWR
Ad-mCherry	Vector Biolabs
PBS, 1X solution, sterile, pH 7,4	VWR
Pellets 17-B-Estradiol 18 mg/ 60 days	Innovative Research of America
Vetbond™ Tissue Adhesive	3M
Petri dishes in polystyrene crystal	Levantina
Penicillin-Streptomycin	Sigma
Syringes, medical 10 ml 0,5 ml	VWR
Nitrile gloves, powder-free	VWR
Soft swiss nude mice	Charles River
Ivis Spectrum In vivo Imaging system	Perkin Elmer
Living Image® (Ivis software)	Perkin Elmer
Fetal Bovine Serum	Gibco
96-well cell culture treated plates	Life technologies
Urine flasks	Summedical
Sterile surgical blades	(Aesculap Division) Sanycare
Isovet 1000 mg/g	B-BRAUN
Buprex® 0.3 mg	Schering Plough S.A.
Injectable morphine solution 10 mg/mL	B BRAUN
Monofyl® Absorbable Sutures	COVIDIEN

Desinclor chlorhexidine

Promedic SA

Microscopy DMI8

Leica Mycrosystems

Hera Cell 150 Incubator

Thermo Scientific

Catalog Number	Comments/Description
22720	Cannula for sampling the uterine endometrium
HYCLSH30285.FS	Medium
1767	Adenoviral vector expressing mCherry
E504-500ML	Buffer for washes
SE-121	Hormone pellets for rodents
780-680	Tissue adhesive
367-P101VR20	Petri dishes
P4333-100ML	Antibiotics
CODA626616	Syringes
112-2754	Gloves
SNUSSFE05S	Mice for animal experiment
124262	In vivo Monitoring equipment
---	In vivo monitoring software
10082147	Enrichment serum
167008	Culture plates
4004-248-001	Flasks for washes
1609022-0008	Surgical blades
---	Isoflurane (Anesthetic)
---	Buprenorphine (Analgesic solution)
---	Morphine (Analgesic solution)
---	Sutures

Antiseptic solution

fluorescence microscope

51026282

Incubator



1 Alewife Center #200
 Cambridge, MA 02140
 tel. 617.945.9051
www.jove.com

ARTICLE AND VIDEO LICENSE AGREEMENT

Title of Article: Noninvasive monitoring of endometriosis progression in a heterologous mouse model.

Author(s): Martínez J, Bisbal V, Marín N, Cano A, Gómez R.

Item 1 (check one box): The Author elects to have the Materials be made available (as described at <http://www.jove.com/author>) via: ☒ Standard Access ☐ Open Access

Item 2 (check one box):

- ☒ The Author is NOT a United States government employee.
- ☐ The Author is a United States government employee and the Materials were prepared in the course of his or her duties as a United States government employee.
- ☐ The Author is a United States government employee but the Materials were NOT prepared in the course of his or her duties as a United States government employee.

ARTICLE AND VIDEO LICENSE AGREEMENT

1. **Defined Terms.** As used in this Article and Video License Agreement, the following terms shall have the following meanings: “**Agreement**” means this Article and Video License Agreement; “**Article**” means the article specified on the last page of this Agreement, including any associated materials such as texts, figures, tables, artwork, abstracts, or summaries contained therein; “**Author**” means the author who is a signatory to this Agreement; “**Collective Work**” means a work, such as a periodical issue, anthology or encyclopedia, in which the Materials in their entirety in unmodified form, along with a number of other contributions, constituting separate and independent works in themselves, are assembled into a collective whole; “**CRC License**” means the Creative Commons Attribution-Non Commercial-No Derivs 3.0 Unported Agreement, the terms and conditions of which can be found at: <http://creativecommons.org/licenses/by-nc-nd/3.0/legalcode>; “**Derivative Work**” means a work based upon the Materials or upon the Materials and other pre-existing works, such as a translation, musical arrangement, dramatization, fictionalization, motion picture version, sound recording, art reproduction, abridgment, condensation, or any other form in which the Materials may be recast, transformed, or adapted; “**Institution**” means the institution, listed on the last page of this Agreement, by which the Author was employed at the time of the creation of the Materials; “**JoVE**” means MyJoVE Corporation, a Massachusetts corporation and the publisher of *The Journal of Visualized Experiments*; “**Materials**” means the Article and / or the Video; “**Parties**” means the Author and JoVE; “**Video**” means any video(s) made by the Author, alone or in conjunction with any other parties, or by JoVE or its affiliates or agents, individually or in collaboration with the Author or any other parties, incorporating all or any portion of the Article, and in which the Author may or may not appear.

2. **Background.** The Author, who is the author of the Article, in order to ensure the dissemination and protection of the Article, desires to have the JoVE publish the Article and create and transmit videos based on the Article. In furtherance of such goals, the Parties desire to memorialize in this Agreement the respective rights of each Party in and to the Article and the Video.

3. **Grant of Rights in Article.** In consideration of JoVE agreeing to publish the Article, the Author hereby grants to JoVE, subject to **Sections 4 and 7** below, the exclusive, royalty-free, perpetual (for the full term of copyright in the Article, including any extensions thereto) license (a) to publish, reproduce, distribute, display and store the Article in all forms, formats and media whether now known or hereafter developed (including without limitation in print, digital and electronic form) throughout the world, (b) to translate the Article into other languages, create adaptations, summaries or extracts of the Article or other Derivative Works (including, without limitation, the Video) or Collective Works based on all or any portion of the Article and exercise all of the rights set forth in (a) above in such translations, adaptations, summaries, extracts, Derivative Works or Collective Works and (c) to license others to do any or all of the above. The foregoing rights may be exercised in all media and formats, whether now known or hereafter devised, and include the right to make such modifications as are technically necessary to exercise the rights in other media and formats. If the “Open Access” box has been checked in **Item 1** above, JoVE and the Author hereby grant to the public all such rights in the Article as provided in, but subject to all limitations and requirements set forth in, the CRC License.

ARTICLE AND VIDEO LICENSE AGREEMENT

4. **Retention of Rights in Article.** Notwithstanding the exclusive license granted to JoVE in **Section 3** above, the Author shall, with respect to the Article, retain the non-exclusive right to use all or part of the Article for the non-commercial purpose of giving lectures, presentations or teaching classes, and to post a copy of the Article on the Institution's website or the Author's personal website, in each case provided that a link to the Article on the JoVE website is provided and notice of JoVE's copyright in the Article is included. All non-copyright intellectual property rights in and to the Article, such as patent rights, shall remain with the Author.

5. **Grant of Rights in Video – Standard Access.** This **Section 5** applies if the "Standard Access" box has been checked in **Item 1** above or if no box has been checked in **Item 1** above. In consideration of JoVE agreeing to produce, display or otherwise assist with the Video, the Author hereby acknowledges and agrees that, Subject to **Section 7** below, JoVE is and shall be the sole and exclusive owner of all rights of any nature, including, without limitation, all copyrights, in and to the Video. To the extent that, by law, the Author is deemed, now or at any time in the future, to have any rights of any nature in or to the Video, the Author hereby disclaims all such rights and transfers all such rights to JoVE.

6. **Grant of Rights in Video – Open Access.** This **Section 6** applies only if the "Open Access" box has been checked in **Item 1** above. In consideration of JoVE agreeing to produce, display or otherwise assist with the Video, the Author hereby grants to JoVE, subject to **Section 7** below, the exclusive, royalty-free, perpetual (for the full term of copyright in the Article, including any extensions thereto) license (a) to publish, reproduce, distribute, display and store the Video in all forms, formats and media whether now known or hereafter developed (including without limitation in print, digital and electronic form) throughout the world, (b) to translate the Video into other languages, create adaptations, summaries or extracts of the Video or other Derivative Works or Collective Works based on all or any portion of the Video and exercise all of the rights set forth in (a) above in such translations, adaptations, summaries, extracts, Derivative Works or Collective Works and (c) to license others to do any or all of the above. The foregoing rights may be exercised in all media and formats, whether now known or hereafter devised, and include the right to make such modifications as are technically necessary to exercise the rights in other media and formats. For any Video to which this Section 6 is applicable, JoVE and the Author hereby grant to the public all such rights in the Video as provided in, but subject to all limitations and requirements set forth in, the CRC License.

7. **Government Employees.** If the Author is a United States government employee and the Article was prepared in the course of his or her duties as a United States government employee, as indicated in **Item 2** above, and any of the licenses or grants granted by the Author hereunder exceed the scope of the 17 U.S.C. 403, then the rights granted hereunder shall be limited to the maximum rights permitted under such

statute. In such case, all provisions contained herein that are not in conflict with such statute shall remain in full force and effect, and all provisions contained herein that do so conflict shall be deemed to be amended so as to provide to JoVE the maximum rights permissible within such statute.

8. **Likeness, Privacy, Personality.** The Author hereby grants JoVE the right to use the Author's name, voice, likeness, picture, photograph, image, biography and performance in any way, commercial or otherwise, in connection with the Materials and the sale, promotion and distribution thereof. The Author hereby waives any and all rights he or she may have, relating to his or her appearance in the Video or otherwise relating to the Materials, under all applicable privacy, likeness, personality or similar laws.

9. **Author Warranties.** The Author represents and warrants that the Article is original, that it has not been published, that the copyright interest is owned by the Author (or, if more than one author is listed at the beginning of this Agreement, by such authors collectively) and has not been assigned, licensed, or otherwise transferred to any other party. The Author represents and warrants that the author(s) listed at the top of this Agreement are the only authors of the Materials. If more than one author is listed at the top of this Agreement and if any such author has not entered into a separate Article and Video License Agreement with JoVE relating to the Materials, the Author represents and warrants that the Author has been authorized by each of the other such authors to execute this Agreement on his or her behalf and to bind him or her with respect to the terms of this Agreement as if each of them had been a party hereto as an Author. The Author warrants that the use, reproduction, distribution, public or private performance or display, and/or modification of all or any portion of the Materials does not and will not violate, infringe and/or misappropriate the patent, trademark, intellectual property or other rights of any third party. The Author represents and warrants that it has and will continue to comply with all government, institutional and other regulations, including, without limitation all institutional, laboratory, hospital, ethical, human and animal treatment, privacy, and all other rules, regulations, laws, procedures or guidelines, applicable to the Materials, and that all research involving human and animal subjects has been approved by the Author's relevant institutional review board.

10. **JoVE Discretion.** If the Author requests the assistance of JoVE in producing the Video in the Author's facility, the Author shall ensure that the presence of JoVE employees, agents or independent contractors is in accordance with the relevant regulations of the Author's institution. If more than one author is listed at the beginning of this Agreement, JoVE may, in its sole discretion, elect not take any action with respect to the Article until such time as it has received complete, executed Article and Video License Agreements from each such author. JoVE reserves the right, in its absolute and sole discretion and without giving any reason therefore, to accept or decline any work submitted to JoVE. JoVE and its employees, agents and independent contractors shall have

ARTICLE AND VIDEO LICENSE AGREEMENT

full, unfettered access to the facilities of the Author or of the Author's institution as necessary to make the Video, whether actually published or not. JoVE has sole discretion as to the method of making and publishing the Materials, including, without limitation, to all decisions regarding editing, lighting, filming, timing of publication, if any, length, quality, content and the like.

11. **Indemnification.** The Author agrees to indemnify JoVE and/or its successors and assigns from and against any and all claims, costs, and expenses, including attorney's fees, arising out of any breach of any warranty or other representations contained herein. The Author further agrees to indemnify and hold harmless JoVE from and against any and all claims, costs, and expenses, including attorney's fees, resulting from the breach by the Author of any representation or warranty contained herein or from allegations or instances of violation of intellectual property rights, damage to the Author's or the Author's institution's facilities, fraud, libel, defamation, research, equipment, experiments, property damage, personal injury, violations of institutional, laboratory, hospital, ethical, human and animal treatment, privacy or other rules, regulations, laws, procedures or guidelines, liabilities and other losses or damages related in any way to the submission of work to JoVE, making of videos by JoVE, or publication in JoVE or elsewhere by JoVE. The Author shall be responsible for, and shall hold JoVE harmless from, damages caused by lack of sterilization, lack of cleanliness or by contamination due to the making of a video by JoVE its employees, agents or independent contractors. All sterilization, cleanliness or decontamination procedures shall be solely the responsibility of the Author and shall be undertaken at the Author's


expense. All indemnifications provided herein shall include JoVE's attorney's fees and costs related to said losses or damages. Such indemnification and holding harmless shall include such losses or damages incurred by, or in connection with, acts or omissions of JoVE, its employees, agents or independent contractors.

12. **Fees.** To cover the cost incurred for publication, JoVE must receive payment before production and publication the Materials. Payment is due in 21 days of invoice. Should the Materials not be published due to an editorial or production decision, these funds will be returned to the Author. Withdrawal by the Author of any submitted Materials after final peer review approval will result in a US\$1,200 fee to cover pre-production expenses incurred by JoVE. If payment is not received by the completion of filming, production and publication of the Materials will be suspended until payment is received.

13. **Transfer, Governing Law.** This Agreement may be assigned by JoVE and shall inure to the benefits of any of JoVE's successors and assignees. This Agreement shall be governed and construed by the internal laws of the Commonwealth of Massachusetts without giving effect to any conflict of law provision thereunder. This Agreement may be executed in counterparts, each of which shall be deemed an original, but all of which together shall be deemed to be one and the same agreement. A signed copy of this Agreement delivered by facsimile, e-mail or other means of electronic transmission shall be deemed to have the same legal effect as delivery of an original signed copy of this Agreement.

A signed copy of this document must be sent with all new submissions. Only one Agreement required per submission.

CORRESPONDING AUTHOR:

Name:	RAÚL GÓMEZ GALLEG0	
Department:	MEDICINA REPRODUCTIVA	
Institution:	INSTITUTO DE INVESTIGACIÓN SANITARIA - INCLIVA	
Article Title:	Noninvasive monitoring of endometriosis progression in a heterologous mouse model.	
Signature:		Date: 06 / 04 / 2018

Please submit a signed and dated copy of this license by one of the following three methods:

- 1) Upload a scanned copy of the document as a pdf on the JoVE submission site;
- 2) Fax the document to +1.866.381.2236;
- 3) Mail the document to JoVE / Attn: JoVE Editorial / 1 Alewife Center #200 / Cambridge, MA 02139

For questions, please email submissions@jove.com or call +1.617.945.9051

TITLE:

Noninvasive Monitoring of Lesion Size in a Heterologous Mouse Model of Endometriosis

AUTHORS & AFFILIATIONS:

Jessica Martínez¹, Viviana Bisbal², Nerea Marín², Antonio Cano^{1,3,4}, Raúl Gómez¹

¹ Instituto de Investigación Sanitaria, INCLIVA, Valencia, Spain

² Unidad de Animalario del Centro de Investigación Príncipe Felipe (CIPF), Valencia, Spain

³ Departamento de Pediatría, Obstetricia y Ginecología, Universidad de Valencia, Spain

⁴ Servicio de Obstetricia y Ginecología, Hospital Clínico Universitario de Valencia, Spain

Corresponding Author:

Raul Gómez (raulgomgal@gmail.com)

Author Email Addresses:

Jessica Martinez (jessik_nenu@hotmail.com)

Vibiana Bisbal (vbisbal@cipf.es)

Nerea Marín (nmarin@cipf.es)

Antono Cano (Antonio.cano@uv.es)

KEYWORDS:

Endometriosis, heterologous, mouse model, mCherry, in vivo, monitoring

SHORT ABSTRACT:

Here, we present a protocol for live-imaging of fluorescently labeled human endometrial fragments grafted in mice. The method allows studying the effects of drugs of choice on endometriotic lesion size through monitoring and quantification of fluorescence emitted by the fluorescent reporter on real time

LONG ABSTRACT:

Here, we describe a protocol for the implementation of a heterologous mouse model in which progression of endometriosis can be assessed in real time through noninvasive monitoring of fluorescence emitted by implanted ectopic human endometrial tissue. For this purpose, biopsies of human endometrium are obtained from donor women ongoing oocyte donation. Human endometrial fragments are cultured in the presence of adenoviruses engineered to express cDNA for the reporter fluorescent protein mCherry. Upon visualization, labeled tissues with an optimal rate of fluorescence after infection are subsequently chosen for the implantation in recipient mice. One week prior to the implantation surgery, recipient mice are oophorectomized, and estradiol pellets are placed subcutaneously to sustain the survival and growth of lesions. On the day of surgery mice are anesthetized, and peritoneal cavity accessed through a small (1.5 cm) incision by the *linea-alba*. Fluorescently labeled implants are tweezed, briefly soaked in glue and attached to the peritoneal layer. Incisions are sutured, and animals left to recover for a couple of days. Fluorescence emitted by endometriotic implants is usually non-invasively monitored every 3 days for 4 weeks with an *in vivo* imaging system. Variations in

the size of endometriotic implants can be estimated in real time by quantification of the mCherry signal and normalization against the initial time-point showing maximal fluorescence intensity.

Traditional preclinical rodents of models of endometriosis do not allow non-invasive monitoring of lesion in real time but rather allow evaluation of the effects of drugs assayed at the end point. This protocol allows one to track lesions in real time and is more useful to explore the therapeutic potential of drugs in preclinical models of endometriosis. The main limitation of the model thus generated is that non-invasive monitoring is not possible over long periods of time due to the episomal expression of Ad-virus.

INTRODUCTION:

Endometriosis is a chronic gynecologic disorder initiated by ~~caused involving~~ the implantation of the functional endometrium outside the uterine cavity. Ectopic lesions grow and induce inflammatory processes ~~provoke grow causing inflammation of the host tissue matation which, inflame~~ leading to chronic pelvic pain and infertility¹. It is estimated that up to ~~Approximately~~ 10%–15% of women of reproductive age are affected by ~~develop~~ endometriosis², and it is present in approximately up to ~~40-50% of infertile of infertile~~ women³. Current pharmacological treatments for endometriosis are unable to completely eradicate lesions and not free of ~~ly, there is not an effective pharmacological treatments eradicating for endometriosis that completely obliterates the lesions without causing~~ side effects^{4,5}. The research for more efficient therapies requires the use of ~~the refinement of the existing~~ animal models of ~~in endometriosis in such a way that which~~ human lesions can be appropriately mimicked, and the effects of compounds on lesion size among others can be closely assessed.

Primate models have been used to mimic endometriosis by implanting ~~induce~~ ectopic lesions that are ~~histologically identical and at similar sites as~~ in humans endometriosis⁶⁻⁸; however, ethical considerations concerns and the high economic costs related to ~~experimentation to experimentation of with experiments using~~ primates limit their use⁹. For this reason ~~Consequently, the use of endometriosis models in~~ small animals, especially rodents, for the implementation of in-vivo models of endometriosis continues to be favored as it allows ~~to allow~~ studies with in large numbers of animals ~~individuals~~^{10,11}. Endometriosis can be induced in these animals by transplanting either pieces of rodent uterine horns (“homologous models”)^{12,13} or human endometrial/endometriotic tissue to ectopic sites (heterologous models)¹⁴. In contrast to humans, rodents do not shed their endometrial tissue and thereby endometriosis can not be ~~do not~~ developed endometriosis ~~spontaneously in these species~~. Therefore, homologous mouse models of endometriosis have been criticized due to the fact that implanted ectopic mouse uterine tissue does not reflect the characteristics of human endometriotic lesions¹⁵.

Appropriate physiology of endometriosis can be mimicked in the heterologous models of endometriosis where fresh human endometrial fragments are implanted into immunodeficient animals. In conventional heterologous models, the therapeutic effects of compounds of interest are commonly assessed at the end point by the assessment of lesion size with the use of

calipers¹⁶. An obvious limitation is that, as such, endpoint animal models do not allow studying implantation dynamics or endometriotic lesion development over time. An additional limitation is that the use of calipers does not allow accurate measurements of lesion size. Indeed, the standard error provided by calipers is in the same range (*i.e.*, millimeters) as the size of the lesions implanted in mice, thus restricting the capacity of these tools to detect actual variations in size.

In order to overcome such limitations, herein, we describe the generation of a heterologous mouse model of endometriosis in which implanted human tissue is engineered to express a reporter m-Cherry fluorescent protein. Detection of the fluorescent signal with an appropriate image system enables non-invasive monitoring of lesion status with simultaneous quantification of its size in real time. Thus, our model provides clear advantages when compared to conventional endpoint models as it brings the opportunity of real-time non-invasive monitoring and the possibility to perform more objective and accurate estimation of variations in lesion size.

PROTOCOL:

The use of human tissue specimens was approved by the Institutional Review Board and Ethics Committee of the Hospital Universitario La Fe. All patients provided written informed consent. The study involving animals was approved by the Institutional Animal Care Committee at the Centro de Investigacion Principe Felipe de Valencia, and all procedures were performed following the guidelines for the care and use of mammals from the National Institutes of Health.

1) Endometrial Tissue Collection and Pre-Processing

1.1) Obtain a good quality biopsy of human endometrial aspirate by using a cannula attached to a suction device. Pour the biopsy into a flask containing 10 mL of sterile saline and wash with gentle manual agitation.

Note: Procedures on how to obtain good quality biopsies have been previously described¹⁷.

1.2) Wash the biopsy of any remaining blood or mucus. Repeat the process by pouring the tissue to flasks containing fresh saline as many times as required until tissue is observed clean.

1.3) Transfer biopsy fragments with a healthy appearance into a solution containing 10 mL of complete Dulbecco's Modified Eagle's medium (DMEM) medium with 10% Fetal Bovine Serum (FBS) and 1% antibiotic-antimycotic solution.

1.4) Pour the content in a 10 cm Petri dish and proceed to chop the tissue into 5-10 mm³ pieces with a pair of scalpels.

2) Adenoviral Transfection of Endometrial Fragments.

Note: All the materials that are going to be employed in the process should be introduced in the hood in advance. Take out everything that is not going to be used in the process and place a flask with bleach. All material that comes into contact with the adenoviral vector must be disinfected with the bleach before discarding it in the biohazard container.

2.1) Once the biopsy has been chopped, take a new Petri dish. Pipette multiple 30-50 μL DMEM drops of spread throughout the whole dish. Leave enough space between drops so they do not come into contact.

2.2) Aided with a needle attached to syringe, place a single piece of fragment inside each of the medium drops.

Note: Each drop should contain a single piece of endometrium.

2.3) Prepare the Ad-mCherry working solution by diluting 1:20 of the mCherry adenoviral stock solution [$1 \cdot 10^{10}$ ifu/mL]) into DMEM medium WITHOUT antibiotics (DMEM + 10% filtered FBS).

2.4) Dispense 100-200 μL of the Ad-mCherry solution per well on a 96-well plate, filling as many wells as fragments are available in the Petri dish drops (step 2.2). In addition, fill at least 3 wells with adenovirus free DMEM medium as a negative control.

2.5) Aided with a needle attached to syringe, transfer each of the fragments in the Petri dish (step 2.2) to each of the wells containing ad-mCherry solution in the 96-well plate.

2.6) Place the 96 well-plate containing the endometrial fragments with Ad-mCherry solution into an incubator at 37 °C with 5% CO_2 for 16 h.

2.7) Wash out the remaining adenoviruses in the medium by transferring tissues into a new 96-well plate filled with complete DMEM medium (WITH antibiotics-antimycotics, free of adenovirus) and incubate for 37 °C with 5% CO_2 for 24-48 h.

NOTE: Remember to cover with bleach all well plates and tips that came in contact with Ad-virus before discarding into the biohazard container.

2.8) Take out the plate from the incubator and place it under a fluorescence microscope at 568 nm (red channel) to test for optimal labeling.

2.9) Choose the most brilliant fragments and place them into a new 96-well plate with fresh complete DMEM medium (WITH antibiotics-antimycotics, free of adenovirus).

2.10) Seal the plate well with a plastic paraffin film and transport it to into the specific-pathogen-free animal area for implantation of endometrial fragments into recipient animals.

3) Generation of the Endometriosis Mouse Model

NOTE: Use 6-8-week-old athymic nude (or similar immunocompromised strains) female mice housed in specific pathogen-free conditions, as recipient animals. To avoid hormonal cycle-dependent variations and simultaneously fuel lesion growth with estradiol, animals are ovariectomized and placed with 60-day release capsules containing 18 mg of 17 β -Estradiol (17 β -E₂). Oophorectomy and pellet placement have to be performed at least one week in advance of grafting endometrial fragments into the recipient animals.

3.1) Oophorectomy

Note: Prepare surgical sterilized material in a hood. Prepare anesthesia equipment and a post-surgical recovery zone ready in the same room.

3.1.1) Perform a subcutaneous injection of morphine derivative at a dose of 5 mg/kg per mouse. Let the mice rest for 30 min after injection so as analgesics effects of drug can be manifested.

3.1.2) Connect the inhalation anesthesia equipment and let oxygen and isoflurane (2% mg/kg) flow for a few min into a sealed anesthesia chamber.

3.1.3) Introduce the animal into the isoflurane anesthesia chamber. Wait for 3-5 min and check that animals are fully anesthetized by pressing one of its paws. Transfer the animal to the surgery area and maintain anesthesia by placing a mask with continuous flow of isoflurane gas covering the respiratory airways.

3.1.4) After disinfecting the area with chlorohexidine, perform a transverse 0.5 cm costal incision approximately at the height of the hip with sharp scissors.

3.1.5) Separate the skin from the muscle to get access to the abdominal cavity, identify the white fat pad that surrounds the ovary and retract the ovary with dissection forceps.

3.1.6) Tie a knot around the oviduct with absorbable suture and tighten it to ensure appropriate hemostasis before excising the ovary.

3.1.7) Close the muscular layer with 6-0 absorbable suture, and then close the skin with 6-0 non-absorbable suture. Clean the area again with antiseptic solution.

3.1.8) Repeat the procedure to remove the contra lateral ovary.

3.2) Estradiol pellet implant

Note: Take care that the animal is anesthetized during the oophorectomy surgery to place

pellets at that point.

3.2.1) Immediately after the completion of the oophorectomy procedure, clean the skin with antiseptic solution surrounding the neck and make a transverse subcutaneous small (0.5 cm) incision with sharp scissors in the nape.

3.2.2) Use the scissors to dissect the skin from the muscle, making a pocket large enough to allow placing the pellets.

3.2.3) Insert the pellet containing 18 mg of 17β -E₂ and suture the skin with a 6-0 non-absorbable suture. Clean the area again with antiseptic solution.

3.2.4) Place the animal in the recovery zone and administer an optimal dose of long-lasting analgesia to ease the recovery period.

3.3) Endometrial implant surgery

NOTE: Allow at least a period of seven days quarantine to allow full recovery of animals after oophorectomy before starting endometrial fragment implantation surgery. For optimal synchronization with labeling of tissue, collect the biopsy 2-3 days before implantation surgery so as to avoid long-term culture of explants.

3.3.1) Get the surgical room in the specific pathogen free zone ready in advance. Prepare the hood with all required surgical material, the anesthesia equipment and the post-surgical recovery zone also.

3.3.2) Bring the animals to the room, perform a subcutaneous injection of a morphine derivative at a dose of 5 (mg/kg) in each mouse. Let the mice rest for 30 min after injection so analgesics effects of drug can be manifested.

3.3.3) Connect the inhalation anesthesia equipment and let oxygen and isoflurane (2% mg/kg) flow for a few min into a sealed anesthesia chamber.

3.3.4) Before starting surgery, move the plate containing fluorescently labeled fragments (from step 2.10) into the hood, unseal it and pour the fragments into a Petri dish for easier handling.

3.3.5) Introduce the animal into the isoflurane anesthesia chamber. Wait for 3-5 min and check that animals are fully anesthetized by pressing one of its paws. Transfer the animal to the surgery area and maintain anesthesia by placing a mask with continuous flow of isoflurane gas covering the respiratory airways.

3.3.5) Place the anesthetized animal face up. Disinfect the ventral area. Perform a longitudinal 1.5 cm incision in abdomen with sharp scissors and separate the skin from the muscle. Then,

perform a longitudinal 1.5 cm incision in the muscle to access the peritoneal cavity.

3.3.6) Hold the left edge of the abdomen muscular wall with mini-forceps and fold it trying to expose the inner face of the peritoneum on the outside.

3.3.7) Take an endometrial implant with mini tweezers, soak it briefly in an n-butyl-ester cyanoacrylate adhesive and place it to the peritoneum where it will get attached. Let it dry for a few seconds. Repeat steps 3.3.6 and 3.3.7 to place an implant on the contralateral side of the peritoneum.

3.3.8) Close the muscular layer with an absorbable 6-0 suture, and then close the skin with a non-absorbable 6-0 suture. Clean the area again with antiseptic solution.

3.3.9) Place the animal in the recovery zone and administer an optimal dose of long-lasting analgesia.

4) *In Vivo* Fluorescent Imaging with an *in vivo* imaging system

4.1) Turn on the *in vivo* imaging system device, initialize the program and allow the CCD camera to cool down for a few min.

4.2) Prepare the inhalation anesthesia equipment. Open the isoflurane flow at 2% for a couple of min to fill the anesthetic chamber. Prepare the post-anesthesia recovery zone.

4.3) Once the program has started and the CCD camera have cooled down, click the **Imaging Wizard** tool: A tutorial starts with a series of consecutive windows displayed, each one corresponding to a parameter of interest with several options available to be chosen by clicking in the corresponding box. Move forward through the tutorial by selecting the appropriate boxes in each window and click the **OK** button to move to the next set of parameters with the following sequence.

4.3.1.) Select the **Epiluminescence box** for the fluorescence parameter, select the **mCherry box** for the filter pairs parameter. Check the **Photograph mode** and **Confirm Focus** boxes and select the Automatic box for the exposure parameter.

4.4) Once the instrument has been set up, move one animal inside the anesthesia chamber. When fully anesthetized, transfer the animal inside the *in vivo* imaging system cage and place it side up with its head inside a tubule connected to the anesthesia machine. Close the lid and click **Acquire** for monitoring.

4.5) Acquire the images appearing (a total of five images, one image for each pair of filters selected) and save data by clicking the **Save As** button. Move the mouse to the area of post-anesthesia recovery. Repeat the process with the remaining animals.

4.6) Repeat monitoring two or three times a week to follow-up the signal appropriately during the time course.

4.7) Proceed to sacrifice the animal at the end of the time course by CO₂ asphyxiation.

5) Quantification of *In Vivo* Fluorescence Images

5.1) Segregation of actual fluorescence through image unmixing:

5.1.1) Open the *In Vivo* Imaging Analysis Coupled Software Program.

5.1.2) Choose the “Sequenceinfo” file to start the analysis. Two windows will appear: “Sequence view” and “Tool Palette”. Choose **Tool Palette** and once the menu has been displayed select the following options.

5.1.3) Select **Corrections** and click on the box **Adaptive FL Background Subtraction** to remove the undesirable fluorescent signals from the luminescent image data. Choose the threshold of greatest interest and click **Set**.

5.1.4.) Click **Spectral Unmixing**, select the wavelengths of interest, the method chosen for unmixing (library, guided, automatic or manual) and then click **Start Unmix**.

5.1.5) Select the **Unmixed** image corresponding to mCherry signal and double click. A new window will appear with the final image of the signal of interest.

5.1.6) Repeat step 5.1.3.

5.1.7) OPTIONAL: If a representative image (JPEG) of the unmix result is needed, choose the desired settings in **Tool Palette | Image Adjust** (color table, binning, contrast, etc.), and then click on **Export Graphics** in the unmix window to export the current image view as an image.

5.1.8) Save the unmixed file: **File | Save As | Choose Folder** and **Ok**.

5.1.9) Repeat the process with the rest of the monitoring days and with all animals.

5.2) ROIs set up and signal quantification

5.2.1) Click **Browse** and select the **Unmixed file** (see step 5.1.8) of interest to be analyzed. A new window will appear.

5.2.2) Click **Add To List** to include all the unmixed files from each animal at different time points and then click on **Load As A Group**. All images must appear as a single sequence.

5.2.3) Go to **Tool Palette** window: Click off the box **Individual** scale to obtain all images on the

same scale.

5.2.4) Double click in one image of the sequence and create a ROI on the zone of interest using the following sequence. Go to **ROI Tools** and select **Countour** and **Auto 1** option, click on the circle shape appearing, place it on the center the fluorescent signal and then click **Create** on the displayed window.

Note: This automatically highlights pixels with an intensity of fluorescence above background values (*i.e.*, lesion) and generates a shape whose area embraces the outlined pixels.

5.2.5) Copy the created ROI shape and paste on a background zone where there is no signal.

5.2.6) Click on **Measure ROIs | Select All** to display values of fluorescence intensity. Proceed to select data values with the mouse, click right button, press copy and paste on a spreadsheet.

6) Data (fluorescent signal) Normalization

6.1) Select the initial time point at which signal intensity is maximal. Proceed to normalize signal at each time point by using the formula:

Signal intensity at each time point / Maximal signal intensity observed during the time course) x 100.

REPRESENTATIVE RESULTS:

Here, we describe the process for creating a heterologous model of endometriosis in which the architecture of lesions is preserved by implanting fluorescently labeled pieces of human endometrium into immunocompromised mice, thus allowing non-invasive monitoring of lesion progression. Labeling of endometrial fragments is achieved by infection with adenovirus engineered to express mCherry, a protein emitting fluorescence in the near infrared region. In **Figure 1**, we show representative images of human endometrial fragments infected with Ad-mCherry observed under the fluorescence microscope. For illustrative purposes, both labeled and non-labeled fragments are included so differences in fluorescence between infected and non-infected tissues (autofluorescence) can be noted. During monitoring, in addition to the reference wavelength for mCherry, fluorescent images are taken with different pairs of excitation/emission wavelengths filters (**Figure 2**) to define the characteristic fluorescent emission profile of tissues. The purpose of this action is to “unmix” actual fluorescence emitted by lesions from background and autofluorescence emitted by host tissues and scar originated during surgery respectively. An illustrative example of the unmix process is shown in **Figure 3**. Estimations of variation in lesion size is performed by quantifying and normalizing fluorescent signaling emitted by lesions during the time course. For this purpose, images of monitoring containing raw fluorescence emitted by animals during each time point are first brought together unnormalized (**Figure 4**) in a single file. Subsequently fluorescence is unmixed, normalized and represented as a false color image (**Figure 5**). Finally, ROIs corresponding to specific lesion and background signaling are automatically recognized by the program and

quantified (**Figure 6**). Background ROI signaling is subtracted from lesion ROI signaling and results of intensity in each time point are normalized against the time point at which intensity is maximal (**Figure 7**). At the end of the monitoring process, several weeks after surgery mice are sacrificed and viable implant can be recovered attached to the mouse peritoneum (**Figure 8**).

FIGURE AND TABLE LEGENDS:

Figure 1: Visualization of endometrial fragments with fluorescence microscope after Ad-mCherry infection **A)** Human endometrial fragment incubated with Ad-mCherry at 37 °C and 5% CO₂ during 24 h as a positive sample. **B)** Human endometrial fragment incubated at 37 °C and 5% CO₂ without Ad-mCherry as a negative control sample.

Figure 2: Raw imaging fluorescence emitted by labeled fragments implanted in mice. Picture shows representative imaging of raw fluorescence signal emitted by the same animal at a specific time point. Images correspond to screenshots obtained using software coupled to an *in vivo* imaging system device during a monitoring session. Each panel containing mice (numbered 1 - 5 in the left corner) corresponds to the fluorescence observed by using a different specific excitation/emission pair filter for acquiring images. Panel on the right (tool palette) show fluorescence parameters selected for acquisition of images

Figure 3: Unmixing of background vs specific fluorescence emitted by lesions. Picture shows representative images of the unmixing process performed to dissect actual fluorescence from lesions using the *in vivo* imaging system coupled software. Graph on the left panel denote normalized specific profiles of fluorescence emission by scar (green line, UMX1), lesions (red line, UMX2) and host tissue (blue line, UMX3 panel). Fluorescence intensity at different emission wavelengths (X-axis) is represented in units of radiant efficiency (Y-axis). Just note how each specific structure (*i.e.*, scar, labeled lesions and host tissue) emits a different fluorescence profile which allows identifying and segregating them specifically from each other. On the right panel, fluorescence arising from launching specific emission profiles for scar (UMX1), lesions (UMX2) and host tissue (UMX3) are shown superposed on photograph images of mice. A composite image (Composite) is also included for illustrative purposes to denote the segmentation of fluorescence emitted by lesions from that emitted by scar or host tissues. Middle panel shows parameters selected for unmixing with the image software coupled to the in-vivo imaging device

Figure 4. Time course monitoring of raw fluorescence emitted by lesions. Panel shows representative images of raw fluorescence emitted by a single mouse implanted with labeled human lesions (brilliant yellow spots) during the time course. Time points after surgery at which monitoring was performed are denoted as “Day (number)”. Emission and excitation pair filters used for monitoring are indicated in each panel/image. Each panel is identified by a specific code (BKG) in the upper part containing info related to the date at which fluorescence was acquired

Figure 5: Time course monitoring of normalized fluorescence emitted by lesions.

Representative images corresponding to unmixed, normalized fluorescent signaling emitted by human lesions (spots with rainbow color) superposed in a single mouse during the time course (days after surgery). Time points after surgery at which monitoring was performed are denoted as “Day (number)”. Each panel is identified by a specific code (BKG) in the lower part containing info related to the date at which fluorescence was acquired. Rainbow palette color on the right side identifies fluorescence intensity (Radiant efficiency) emitted by lesions at each time point. Note how strong fluorescence intensity during the initial time points (*i.e.*, red color in the center of lesions on days 1,5 and 8) declines during the time course (*i.e.*, blue color in lesions on days 20 and 25).

Figure 6: Use of ROIs for quantification of fluorescence intensity in lesions during the time course. Figure shows panel of images of normalized fluorescence emitted by lesions in a single mouse during the time course (*i.e.*, **Figure 5**) with the addition of ROIs (delineating lesions and background) for quantification of fluorescence intensity. ROI 1 and ROI 2 identify the amount of fluorescence emitted by each of the two lesions during the time course. BKG identify the amount of fluorescence emitted by the host tissue (background fluorescence) during the time course. Background fluorescence is subtracted from ROIs for quantification purposes. Time points after surgery at which monitoring was performed are denoted as “Day (number)”. Images acquired at each time point are labeled with a specific code (BKG) at the bottom of each one containing info related to the date at which fluorescence was acquired (first eight digits following BKG detail data for year(2014)-month (10) and -day(10 to 31)), an individual identification code (last 6 digits) and the specific profiles of fluorescence emission used for unmixing (UMX2) Rainbow palette color on the right side provides a visual scale of fluorescence intensity (Radiant efficiency) emitted by lesions at each time point. Note how fluorescence intensity values in the two lesions (ROI1 and ROI2) are higher at the initial time points (days 1 and 5) and decays during the time course to reach the lowest values at the end time points (days 20 and 25).

Figure 7: Normalization of fluorescence intensity during the time course. Table in the upper part shows illustrative example of the values of fluorescence intensity (radiant efficiency) emitted by two mCherry labeled lesions (ROI1 and ROI2) implanted in a mouse (R25). Monitoring of fluorescence was performed at different days after surgery (D5-D25) during the time course. D5- Graph at the bottom illustrates typical pattern of normalized fluorescence emitted by lesions infected with mCherry decaying during the time course. Y-axis shows values of fluorescence normalized to express the percentage of decay by using the formula (Signal intensity at each time point / Maximal signal intensity observed during the time course) x 100. Time points (Days (Dx) after implanting surgery) at which fluorescence was monitored are indicated in the X-axis. Note initial increase of signaling during the first 24 hrs after surgery, corresponding to stabilization of lesion, the peak in fluorescence intensity around D1-D5 and its subsequent decay due to episomal expression of mCherry during the time course

Figure 8: Macroscopic appearance of implanted endometriotic lesions. Representative images showing macroscopic appearance of endometriotic lesions implanted in mice at the end of the monitoring process upon sacrifice

DISCUSSION:

The protocol herein detailed describes the implementation of an animal model of endometriosis in which the architecture of implanting lesions architecture is preserved whilst simultaneously allowing real time assessment of fluorescence emitted by mCherry labeled endometrial tissue. In this protocol, we describe the use of a specific *in vivo* imaging system and related software to non-invasively assess fluorescence emitted by the labeled lesion. Each user should adapt the protocol depending on the specific imaging device and related software available at their institution. Monitoring is performed in anesthetized animals through an isoflurane gas anesthesia machine coupled to an *in vivo* imaging system. To avoid interference with auto-fluorescence emitted by wounds, it is recommended to start monitoring lesions fluorescence at least three days after implantation surgery.

Heterologous mouse models of endometriosis similar to the one herein shown have been previously described consisting in the implantation endometrial fragments labeled with green fluorescent protein (GFP)^{18,19}. The use of mCherry as a reporter for tagging the human tissue provides however an advantage over GFP because of the enhanced tissue penetration of the former. Due to its larger emission spectrum and higher photostability mCherry emits a brighter signal that is more appropriate for the visualization of intraperitoneal fragments.

Due to its small size adenoviruses are the vectors of choice for infection (*i.e.*, labeling) of whole tissue pieces as those provide acceptable diffusion through 3D structures. Even with that the percentage of tissue infected cells is not higher than 30-35%. Thus, the limitation of this model relies on the inefficient labeling of tissue and additionally the transient expression achieved by adenoviruses. Indeed, fluorescence cannot be monitored beyond 4–6 week as it fades progressively due to the episomal transient expression of the Ad-virus. Efficiency of labeling and the period of monitoring might be increased by disrupting the donor tissue and infecting isolated single epithelial/stromal cells with ad-virus previous to being injected into recipient mice^{19,20}. Such an approach, however, reduces the extent at which the animal model mimics the physiology of endometriosis provided that ectopic human lesions do not consist in a disorganized accumulation of single epithelial/stromal cells but rather in well-structured endometriotic tissue.

In this protocol, the most critical step is the labeling of the tissue and most specifically the determination of the appropriate concentration of ad-virus required for optimal infection. Indeed, the 1×10^{10} pfu/mL concentration pointed out in the protocol is mostly an orientative/consensus figure based on our experience. The optimal concentration might differ in each experiment depending on the type and quality of the biopsy and/or how quickly this is processed. We thus suggest testing at least three different (two-fold) titers in each experiment and choosing the one providing optimal labeling based on visualization under the fluorescence microscope.

Our protocol/model is useful to study the mechanisms implicated in the establishment and early development of the endometriotic lesions. In spite of the period of time of monitoring is

constrained, the model is still useful to study and detect the effects of pharmacological compounds able to exert dramatic effects on lesion size in a short period of time such as antiangiogenic or antiestrogenic drugs. The development of more efficient and durable methods of labeling human tissue are expected to spread non-invasive monitoring as a consolidated technique to explore the potential therapeutic of a wider range of drugs in preclinical model endometriosis.

ACKNOWLEDGMENTS:

This work was supported by Spanish Ministry of Economy and Competitiveness through the Miguel Servet Program [CP13/00077] cofounded by FEDER (European Regional Development Fund) and awarded to Dr R. Gómez as well as by Carlos III Institute of Health grants awarded to Dr R Gómez [PI14/00547 and PI17/02329] and to Prof A. Cano [PI12/02582].

DISCLOSURES:

The authors have nothing to disclose.

REFERENCES:

1. Nap AW, Groothuis PG, Demir AY, Evers JL, Dunselman GA. Pathogenesis of endometriosis. *Best Practice & Research: Clinical Obstetrics & Gynaecology*; **18**, 233–244 (2004).
2. Holoch KJ, Lessey BA. Endometriosis and infertility. *Clinical Obstetrics and Gynecology*; **53**, 429–438 (2010).
3. Eskenazi B, Warner ML. Epidemiology of endometriosis. *Obstetrics and Gynecology Clinics of North America*; **24** (2), 235–258 (1997).
4. Giudice LC, Kao LC. Endometriosis. *Lancet*; **364** (9447), 1789–1799 (2004).
5. Donnez J, *et al.* The efficacy of medical and surgical treatment of endometriosis-associated infertility and pelvic pain. *Gynecologic and Obstetric Investigation*; **54**, 2–7 (2002).
6. D’Hooghe TM, Bambra CS, Cornillie FJ, Isahakia M, Koninckx PR. Prevalence and laparoscopic appearance of spontaneous endometriosis in the baboon (*Papio anubis*, *Papio cynocephalus*). *Biology of Reproduction*; **45** (3), 411–416 (1991).
7. Dick EJ, Hubbard GB, Martin LJ, Leland MM. Record review of baboons with histologically confirmed endometriosis in a large established colony. *Journal of Medical Primatology*; **32** (1), 39–47 (2003).
8. Donnez O, *et al.* Induction of endometriotic nodules in an experimental baboon model mimicking human deep nodular lesions. *Fertility & Sterility*; **99** (3), 783–789 (2013).
9. Grummer R. Animal models in endometriosis research. *Human Reproduction Update*; **12** (5), 641–649 (2006).
10. Rossi G, *et al.* Dynamic aspects of endometriosis in a mouse model through analysis of implantation and progression. *Archives of Gynecology and Obstetrics*; **263** (3), 102–107 (2000).
11. Grummer R, *et al.* Peritoneal endometriosis: validation of an in-vivo model. *Human Reproduction*; **16** (8), 1736–1743 (2001).
12. Becker CM, *et al.* A novel non-invasive model of endometriosis for monitoring the efficacy of antiangiogenic therapy. *The American Journal of Pathology*; **168** (6), 2074–2084 (2006).

13. Laschke MW, Giebels C, Nickels RM, Scheuer C, Menger MD. Endothelial progenitor cells contribute to the vascularization of endometriotic lesions. *The American Journal of Pathology*; **178** (1), 442-450 (2011).
14. Nap AW, *et al.* Antiangiogenesis therapy for endometriosis. *The Journal of Clinical Endocrinology & Metabolism*; **89** (3), 1089-95 (2004).
15. Wang CC, *et al.* Prodrug of green tea epigallocatechin-3-gallate (Pro-EGCG) as a potent anti-angiogenesis agent for endometriosis in mice. *Angiogenesis*; **16** (1), 59–69 (2013).
16. Delgado-Rosas F, *et al.* The effects of ergot and non-ergot-derived dopamine agonists in an experimental mouse model of endometriosis. *Reproduction*; **142** (5), 745-55 (2011).
17. Al-Jefout M, Andreadis N, Tokushige N, Markham R, Fraser I. A pilot study to evaluate the relative efficacy of endometrial biopsy and full curettage in making a diagnosis of endometriosis by the detection of endometrial nerve fibers. *American Journal of Obstetrics & Gynecology*; **197** (6), 578 (2007).
18. Fortin M, *et al.* Quantitative assessment of human endometriotic tissue maintenance and regression in a noninvasive mouse model of endometriosis. *Molecular Therapy*; **9** (4), 540-7 (2004).
19. Liu B, *et al.* Improved nude mouse models for green fluorescence human endometriosis. *Journal of Obstetrics and Gynaecology Research*; **36** (6), 1214-21 (2010).
20. Wang N, *et al.* A red fluorescent nude mouse model of human endometriosis: advantages of a non-invasive imaging method. *European Journal of Obstetric Gynecologic and Reproductive Biology*; **176**, 25-30 (2014).